LBL-10564 C.2
Preprint

Lawrence Berkeley Laboratory
UNIVERSITY OF CALIFORNIA

Materials & Molecular Research Division

Submitted to the Journal of Chemical Physics

STUDY OF THE REACTION DYNAMICS OF Li + HF, HCl
BY THE CROSSED MOLECULAR BEAMS METHOD

Christopher H. Becker, Piergiorgio Casavecchia,
Peter W. Tiedemann, James J. Valentini, and Yuan T. Lee

May 1980

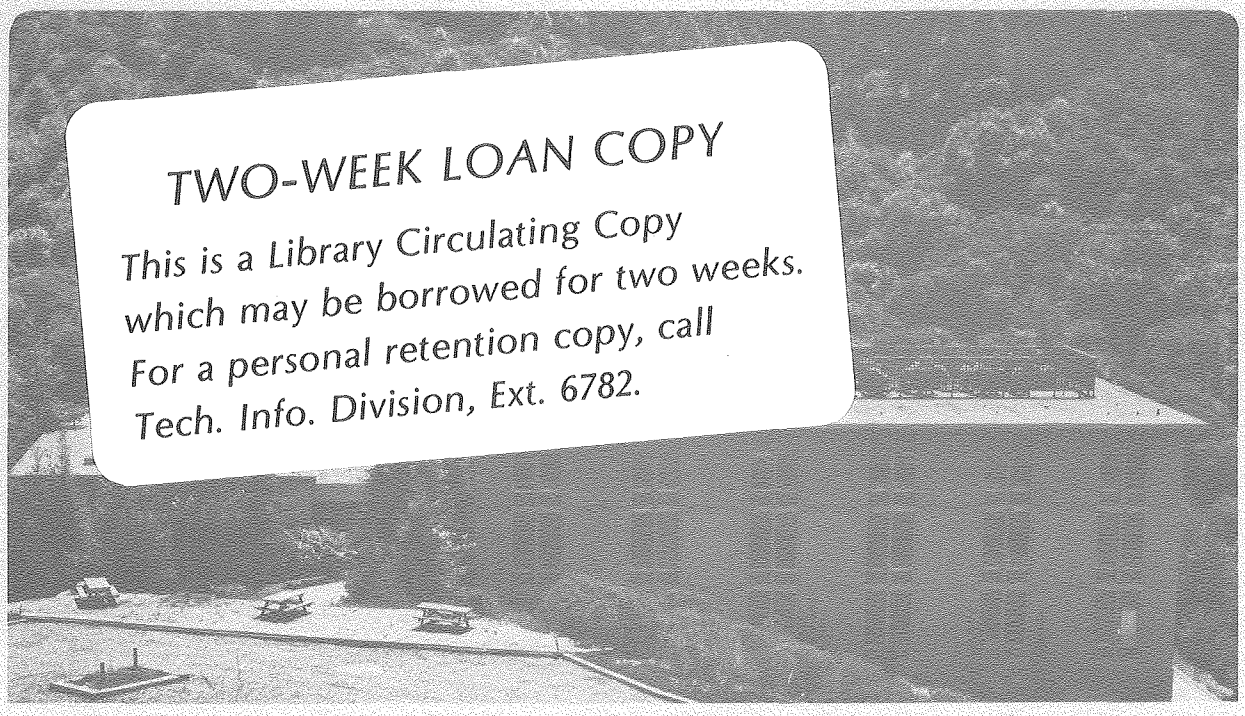

Prepared for the U.S. Department of Energy under Contract W-7405-ENG-48

DISCLAIMER

LBL-10564

STUDY OF THE REACTION DYNAMICS OF Li + HF, HCl BY THE CROSSED MOLECULAR BEAMS METHOD

Christopher H. Becker[a], Piergiorgio Casavecchia[b], Peter W. Tiedemann[c], James J. Valentini[d], and Yuan T. Lee

Materials and Molecular Research Division
Lawrence Berkeley Laboratory

and

Department of Chemistry
University of California
Berkeley, California 94720

MAY 1980

ABSTRACT

The reactions of (I) Li + HF → LiF + H and (II) Li + HCl → LiCl + H have been studied by the crossed molecular beams method. Angular distributions [$N(\Theta)$] of product molecules have been measured at 4 collision energies (E_c) ranging from about 2 to 9 kcal/mole and time-of-flight (TOF) measurements of product velocity distribution were made at approximately E_c = 3 and 9 kcal/mole for both reactions (I) and (II). The combined $N(\Theta)$ and TOF results were used to generate contour maps of lithium-halide product flux in angle and recoil velocity in the

---

[a]Present address: Department of Chemistry, Massachusetts Institute of Technology, Cambridge, Massachusetts 02139.

[b]Permanent address: Dipartimento di Chimica dell'Universita, 06100 Perugia, Italy.

[c]Permanent address: Instituto de Quimica, Universitade de Sao Paulo, C.P. 20780, Sao Paulo, Brazil.

[d]Permanent address: Los Alamos Scientific Laboratory, P. O. Box 1663, Los Alamos, New Mexico 87545.

center-of-mass (c.m.) frame. For reaction (I) at E_c = 3 kcal/mole the c.m. angular distribution [$T(\theta)$] shows evidence of complex formation with near forward-backward symmetry; slightly favored backward peaking is observed. The shape of this $T(\theta)$ indicates there is significant parallel or antiparallel spatial orientation of initial and final orbital angular momentum $\vec{L}$ and $\vec{L}'$, even though with H departing L' must be rather small and $\vec{L} \simeq \vec{J}'$, where $\vec{J}'$ is the final rotational angular momentum vector. It is deduced that coplanar reaction geometries are strongly favored. At E_c = 8.7 kcal/mole the $T(\theta)$ of reaction (I) becomes strongly forward peaked. The product translational energy distributions $P(E_T')$ at both these collision energies give an average E_T' of ~55% of the total available energy; this appears consistent with a theoretically calculated late exit barrier to reaction. The $T(\theta)$ at E_c = 2.9 and 9.2 kcal/mole for reaction (II) are forward-sideways peaked. Most of the available energy (~70%) goes into recoil velocity at both E_c for LiCl formation. This suggests a late energy release for this 11 kcal/mole exoergic reaction. Both reactions (I) and (II) show evidence of no more than a minor partitioning of energy into product vibrational excitation. Integral reactive cross sections (σ_R) are evaluated by integrating the product distributions in the c.m. frame and using small angle nonreactive scattering of Li as an absolute calibrant. Values of σ_R are: for LiF formation $\sigma_R \simeq 0.8$ Å^2 and 0.94 Å^2 at E_c = 3 and 8.7 kcal/mole, while for LiCl formation σ_R = 27 Å^2 and 42 Å^2 at E_c = 2.9 and 9.2 kcal/mole, with estimated absolute and relative uncertainties of a factor of 2, and 30%, respectively. Average opacities for reaction have been estimated from

the reaction cross sections and the extent of rotational excitation of products to be about 0.1 for reaction (I) and 1 for reaction (II), for L values allowed to react. These results are discussed in some detail with regard to the kinematic constraints, reaction dynamics and potential energy surfaces for these two reactions, and related experimental and theoretical work are noted.

In addition, angular distributions of nonreactive scattering of Li off HF and HCl are measured at 4 different E_c each. Rainbow structure is observed at low E_c and the angular distributions are fit by a spherically symmetric piecewise analytic potential. The resulting values of the potential's well depth (ε) and minimum position (r_m) are: for Li + HF ε = 0.46 kcal/mole and r_m = 4.34 Å and for Li + HCl ε = 0.32 kcal/mole and r_m = 4.7 Å. These results differ significantly from some earlier estimates based on the measurements of integral scattering cross sections.

I. INTRODUCTION

Crossed molecular beams studies of reactive and nonreactive scattering of the systems $Li(^2S_{1/2}) + HX(^1\Sigma^+, v=0)$ (X = F, Cl) have been carried out at collision energies ranging from approximately 2 to 9 kcal/mole under single collision conditions. These studies have been motivated by a desire to increase our understanding of elementary chemical processes in several ways.

As a direct consequence of experimental measurements, information is obtained about the dynamics of these two particular reactions involving lithium atoms and hydrogen halides. A more far reaching motivation is to provide experimental results for a future test of the accuracies of *ab initio* and semi-empirical potential energy surfaces and reactive scattering computational methods and to allow examination of the correlation between the potential energy surface (PES) of a system and the reaction dynamics, for a given mass combination. The Li + HF system is a good test case because of the simplifications of dealing computationally with only these light atoms, only one reactive product channel, LiF + H, is energetically open, and only one PES governs the dynamics at collision energies up to ~30 kcal/mole.

A partial PES for Li-F-H was first computed by *ab initio* means by Lester and Krauss.[1] Only the entrance channel of Li + HF was examined. A particularly interesting result found was the significant attraction of 3.6 kcal/mole for a linear Li-F-H configuration, deepening slightly for a more bent configuration. The interpretation of the origin of this attraction was ambiguous; it could be due either to a surprisingly

strong electronic $^2S_{1/2}$-$^1\Sigma^+$ interaction for a stable triatomic configuration or simply to the onset of the chemical reaction.

Evidence of a rather strongly bound triatomic system for Li-F-H, but not Li-Cl-H, was put forth by Trenary et al.[2] in a fascinating ab initio study of Li and Na with first and second row diatomic hydrides. The dissociation energy of the constrained linear LiFH → Li + HF was estimated to be 4.2 kcal/mole, compared to the reaction exoergicity of 1.1 kcal/mole. Semiempirical PES have been reported for LiFH by Balint-Kurti and Yardley,[3] for LiFH[4,5] and LiClH[5] by Zeiri and Shapiro. Another more complete ab initio PES for LiFH recently has been carried out by Chen and Schaefer.[6] Two of the more extensive semiempirical and recent ab initio PES calculations on Li + HF also show the existence of a stable LiFH configuration with D_e values of 2.5 kcal/mole[3] (for Li-F-H angle of 135°) and 4.6 kcal/mole[6] (for 114°), differing from that shown in Figs. 5 and 8 of reference 4. These studies also show the existence of an exit potential energy barrier for breaking H atom from LiF. At a bent configuration the height of the barrier of LiFH is smallest and is calculated to be 10.4 kcal/mole,[3] 12.4 kcal/mole,[5] and 10.0 kcal/mole[6] relative to the potential minimum for Li + HF. If the zero point energies are taken into account, the last value becomes 6.4 kcal/mole.[6]

In one previous molecular beam experimental study[7] of Li + HF, HCl, nonreactive integral cross sections were measured as a function of Li velocity. Partially quenched glory oscillations were seen for Li + HCl, but not for Li + HF, and by assuming a spherically symmetric interaction with

a Lennard-Jones (12-6) potential, values of εr_m, ε, and r_m were determined, where ε and r_m are the well depth and the position of the potential minimum, respectively. The product εr_m is in principle better determined in the analysis of the glory oscillations than ε and r_m independently. Results were for HF: ε = 0.10 kcal/mole and r_m = 4.79 Å, and for HCl: ε = 0.51 kcal/mole and r_m = 4.02 Å. For HF, these values differ somewhat from a calculated spherical averaged interaction potential by Lester and Krauss[1] (ε = 0.06 kcal/mole, r_m = 5.0 Å).

There are several recent reviews of computational methods for reactive scattering.[8,9,10] Fully quantum mechanical calculations might not likely be carried out for the Li-HX systems in the very near future due to the large number of channels involved. Classical trajectory methods are by far the most common for such systems. Because LiCl formation is exoergic by ~11 kcal/mole and is found to be facile, the classical trajectory methods are likely to be adequate for obtaining some important features of reaction dynamics from the potential energy surface. The question of H tunneling through the exit barrier in LiF formation at low collision energy which cannot be described adequately by classical trajectory methods, can provide an important test of approximate quantum methods.[11-13] One scattering calculation has been carried out based on the consideration of coupling coefficients between reactant and product angular momentum functions without using a PES for Li + HF[14] reflecting the consequences of kinematic constraints for this system.

From a more historical perspective on alkali atoms with hydrogen halides, K + HBr → KBr + H was the first successful crossed molecular beams experiment, in 1955.[15] Unfortunately, little detailed dynamical information was obtained for this system primarily due to the kinematic constraint forcing the product KBr to travel very close to the center of mass velocity vector.[16,17] During the 1960's the reactive[18] and nonreactive[19,20] scattering of K + HBr continued to receive extensive attention from several groups. With some improvements in apparatus, the center-of-mass (c.m.) angular distributions, $T(\theta)$, and product translational energy distributions, $P(E_T')$, were obtained for K + HBR, DBr[18] and a rough $T(\theta)$ deduced for K + TBr.[21]

Most recently, the effect of reagent translational and vibrational energy on the reaction K + HCl → KCl + H has been studied,[22] though no attempt was made to determine the angular and energy distributions of scattered products in the c.m. system. This study has shown a drastic increase in reaction probability with vibrational excitation for this slightly endoergic reaction, while the equivalent amount of translational energy was found to be much less effective in promoting this chemical reaction.

From a study of the family of reverse reactions (H + MX → HM + X)[23,24] it was found that these reactions have very small barriers, the c.m. angular distributions are quite anisotropic, and the reactive cross sections are modest (1-10 $\mathring{A}^2$). But the conclusions derived were quite uncertain, due to the poor resolution of the experiments using high temperature beams with thermal velocity distributions.

The electric deflection analysis of the CsBr product from the Cs + HBr reaction,[25,26] has indicated that essentially all of the available angular momentum goes into product rotation, as expected for this family of reactions.[27] Recently the reactivity as a function of the reactant rotational state has been investigated for K + HCl (v = 1,J);[28] this experiment suggests that molecular rotation inhibits reactions. The general effect of the rotational excitation of the reactants on the reactivity is still not well understood.[29] A nonmonotonic effect has been reported for the Na + HX reaction.[30]

In this study in order to understand the interaction potentials and reaction dynamics of Li + HF and Li + HCl high resolution crossed molecular beams experiments have been performed. After a description of the experimental conditions in Sect. II, we present the experimental measurements of nonreactive and reactive angular distributions for the Li + HF and Li + HCl systems at four different collision energies, and also the results of the time-of-flight velocity measurements of the reaction product at two energies for each system in Sect. III. The methods of analysis of the reactive scattering data are briefly discussed in Sect. IV, and the results of the analysis are given in terms of the c.m. angular and translational energy distributions of products. Also in Sect. IV, an estimate of the nonreactive integral cross section is given, and the nonreactive angular distributions are analyzed in terms of the spherically symmetric part of the potential for the Li + HF and Li + HCl interactions. In Sect. V therse results are discussed, with particular reference to the information they contain about the

relation between PES, kinematic constraints and dynamics for these reactions.

II. EXPERIMENTAL ARRANGEMENT

The crossed molecular beam apparatus employed in this study has been described in detail previously.[31,32] Supersonic beams of Li atoms seeded in a rare gas carrier and of HF (HCl) molecules, after differential pumping stages, are crossed under single collision conditions at 90° in a liquid nitrogen cooled collision chamber maintained at ~1.5 x 10^{-7} torr. The Li source consists of a tantalum reservoir with a gas inlet tube and a tantalum nozzle tube attached by electron beam welding. The reservoir is radiatively heated by a 0.05 mm x 2.0 mm tungsten ribbon wound around eight high purity alumina posts, which are surrounded by three tantalum radiation shields. The reservoir temperature is monitored with a thermocouple spot-welded to the bottom of the reservoir. About 450 watt are dissipated in this heater for attaining a temperature of 960°C, which corresponds to a lithium vapor pressure of 27 torr. The nozzle tube is heated in a similar way (except that the heater is smaller - four alumina posts are used); with 170 watts a temperature of 1150°C is attained. The temperature of the nozzle must be considerably higher than that of the reservoir in order to avoid Li_2 formation in the beam and Li condensation at the nozzle. Search for Li_2 in the Li beams has indicated their absence in our experimental conditions. Various rare gas mixtures with different average mass number could be flowed into the reservoir as carrier gases through the inlet tube allowing one to vary the Li atom velocity

by the seeded beam technique, and thus vary the collision energy. The rare gas pressure is usually 1200 torr. The inlet tube has a constriction just before entering the reservoir to ensure a local high gas velocity which prevents lithium from backstreaming, and there is a baffle inside the reservoir to ensure thorough mixing of the lithium vapor and carrier gas. The skimmer attached to the beam source chamber is constructed as a one-piece skimmer-heater unit, and heated to 500°C to prevent lithium condensation at the skimmer orifice. It is not necessary to heat the defining slit which follows the skimmer, since the amount of lithium deposition is small even after two weeks of operation. The supersonic lithium beam, produced from a 0.08 mm diameter nozzle, is defined to a 2.3° angular divergence, giving a beam width of 3 mm at the collision center.

A supersonic HF (HCl) beam is produced from an oven/nozzle source, which is a resistively heated nickel tube, maintained at 380°C to prevent HF (HCl) dimer formation. At this temperature, the concentration of the dimers monitored by the mass spectrometer as H_2F^+ and H_2Cl^+ are found to be less than 1% of the monomer. The nozzle diameter is 0.08 mm and the angular divergence of the beam ~3.5°, also giving a beam width of 3 mm at the collision center. HF and HCl are research grade from Matheson Gas Products and are not further purified. A cylinder of pure hydrogen fluoride was kept at room temperature so as to yield a stagnation pressure of 740 torr behind the nozzle. Pure hydrogen chloride was used with a pressure regulator to give a stagnation pressure of 800 torr.

The velocity distributions of the beams are characterized by time-of-flight (TOF) measurement and Table I gives the Li, HF and HCl molecules effective bulk flow temperature, Mach number, full-width-at-half-maximum (FWHM) relative velocity spread and peak velocity. Also shown are the four average collision energies (E_c) for the Li + HF and Li + HCl systems. Typical velocity distributions of the beams are shown in Fig. 1. The solid line is a parametric fit to the deconvoluted distribution for the Mach number and the temperature given in Table I.

Angular distributions of reactively scattered LiF and LiCl, and elastically or inelastically scattered Li are measured in the plane defined by the two beams as a function of laboratory scattering angle, Θ, measured from the Li beam by a rotatable ultrahigh vacuum mass spectrometric detector.[31] The angular distribution measurements are time normalized by periodically returning the detector to an arbitrary angle chosen as reference during the scan in order to account for possible long term drifts in beam intensity and detector sensitivity. Modulated background near the hydrogen halide beam ($\leq 15°$) is corrected by counting for equal time with the primary beam flag open and closed, and subtracting the results. The amount of this correction varies from a few per cent at $\Theta = 75°$ to a maximum of 60% at $\Theta = 84°$ for LiF produced in the Li + HF reaction at $E_c = 2.2$ kcal/mole.

Velocity distributions of the incident beams are determined by conventional TOF measurements, with the detector aperture reduced from the normal 3 x 4 mm to 0.13 mm diameter to allow a shorter shutter opening period and maintain a low detector pressure. A chopper disc of 17.8 cm

diameter rotating at 290 Hz with eight 1 mm wide slots is used for all Li, HF and HCl beams. This provides a 6 μsec shutter opening period. The data is recorded with a 255 channel multiscaler operating at 2 μsec dwell time per channel.

Product velocity distributions at selected angles are determined by means of two different TOF methods, depending on the signal-to-noise (S/N) ratio. For the highest S/N ratio of scattered product (for Li + HCl at E_C = 9.2 kcal/mole) conventional TOF measurements are performed, similar to the determination of the beam velocity distribution, except with a 3 x 1 mm entrance slit. For LiCl scattered from Li + HCl at E_C = 9.2 kcal/mole, the flight times from chopping wheel to the detector range from 110 to 240 μsec; the shutter opening period is 2.5 to 5.5% of the flight time for this system. This is smaller than the 9% dispersion of length of flight path (17 cm) due to the finite length of the ionization region (1.5 cm). When S/N ratios are low, product velocity distributions are determined by means of the cross correlation (CC) time-of-flight technique.[33] For these measurements the product molecules are modulated at the detector entrance aperture (3 x 2.2 mm) by a rotating wheel, the periphery of which is coded with a pseudo-random binary sequence of open and closed slots (255 elements). The wheel diameter is again 17.8 cm and the width of each element is 2.2 mm. The efficiency of signal recovery is improved by a factor of ~35 for the CC method compared with the conventional TOF method described above, due to the higher fractional open time (~50%) of the pseudo-random chopper compared with that (~1.4%) of the conventional chopper

disc. The CC disc rotates at 326.8 Hz, corresponding to a shutter function of 12 μsec for each element of the pseudo-random sequence. On-line minicomputer control and data reduction is used to allow immediate recovery of the time-of-flight distribution of the product by cross correlating the modulation function with the measured spectrum recorded by the 255 channel scaler. The channel width of the multichannel analyzer is 12 μsec, identical to the opening time of the smallest slot of the CC disc. Thus at the flight time of our experiment the CC chopper gives a time resolution of 5-11%. The uncertainty in the laboratory velocity distributions of the products caused by both time resolution and flight path dispersion is accounted for in the data analysis, performing a deconvolution of the TOF spectra over the ionizer length, as well as over the finite slit sizes of the TOF wheel and of the detector.

Aside from the fact that the signal from the electron bombardment ionization detector is proportional to the number density of atoms or molecules in the ionizer, it is also proportional to the ionization cross section and fragmentation pattern of a given specie and the transmission of the mass spectrometer. The ratios of mass to charge values m/e 7:42 and 7:26 which give information on the ions coming from dissociative and direct ionization of the $^{7}Li^{35}Cl$ and $^{7}Li^{19}F$ by 200 eV electrons have been measured at the peak of the reactive angular distributions at different collision energies. The contribution to Li^{+} coming from nonreactively scattered Li atoms has been taken into account at the peak angle by interpolating the rather smooth and monotonic

nature of the nonreactive Li angular distributions in these ranges (see Sect. III). The following values of ratios of the observed signal have been obtained: m/e 7:42 = 1.9:1 and 7:26 = 5.7:1. The relative mass dependent transmission function of the quadrupole has been determined from the known fragmentation pattern of trans-2-butene.[34] The following relative values of transmission have been obtained (the index indicates the mass in amu): $f_7 = 1$, $f_{26} = 0.58$, $f_{42} = 0.24$. From the above ratios of m/e and from the determined transmission function, the branching ratios for the ionization process for LiF and LiCl are derived: $Li^+/LiF^+ = 3.3$; $Li^+/LiCl^+ = 0.34$. The latter was corrected for isotopic contributions. These values are very close to the results of mass spectrometric investigations of the fragmentation of the LiX vapor system at high temperatures. Li^+/LiX^+, from the LiX, was reported to be 3.5 for X = F[35] and 0.30 for X = Cl[36] at an electron energy of 75 eV.

The laboratory angular distributions of LiCl are measured at m/e = 42, using counting times between 10 sec (at E_C = 9.2 kcal/mole) and 40 sec (at E_C = 1.9 kcal/mole) at each angle, giving a S/N ratio of 100 and 35 at the peak of the distributions, respectively. Angular distributions of LiF product are recorded at m/e = 26 only at the two highest collision energies, namely E_C = 8.7 and 5.7 kcal/mole. With 60 seconds counting time, S/N is 15 and 9 respectively. Product counting rates at the peak of the angular distribution for m/e = 42 and m/e = 26 were typically 1850 cts/sec and 60 cts/sec for the experiments with highest collision energies. At the two lowest

collision energies signals at m/e = 26 for LiF are too low, thus the angular distributions of LiF are obtained from the m/e = 7 angular distributions (see Sect. III). Typical counting times for the m/e = 7 angular distributions are between 20 sec and 60 sec for both systems at the highest and lowest collision energy, respectively. A total of 4 to 6 scans are carried out for each angular distribution measurement.

The velocity distributions of the LiF and LiCl products are obtained at m/e = 7, taking advantage of the favorable branching ratio and higher transmission of Li^+. Since the reactively scattered LiX and nonreactively scattered Li have distinctly different laboratory velocities, the TOF data is capable of distinguishing between reactive and nonreactive m/e 7 signals. At E_C = 9.2 kcal/mole the m/e = 42 LiCl TOF spectra also were recorded at m/e = 42 in order to check the m/e = 7 data. The TOF peak corresponding to elastically scattered lithium is not detectable at a large scattering angle for the Li + HCl system where reactive signals are dominating, indicating a very large depletion of nonreactive lithium intensity due to chemical reaction, while the elastic signal is present and distinct for the Li + HF system at all angles. Typical recording times are 90 minutes at each angle for the conventional TOF of Li^+ from LiCl at E_C = 9.2 kcal/mole and 5 to 60 minutes for the cross correlation TOF of Li^+ from LiCl and LiF at the other energies studied.

III. EXPERIMENTAL RESULTS

The velocity distributions of the reactants measured by the TOF method are shown in Fig. 1. The solid circles are the data transformed from time to velocity space and the line is the best fit distribution convoluted over the experimental resolution. The parameters which describe the fitted distributions are those of Table I. An exemplary Newton diagram displaying a kinematic system is shown in Fig. 2. The effect of the velocity spreads of reactants has been indicated in Fig. 2 by drawing two more Newton diagrams about the nominal velocity vectors - the most probable values. The extreme velocities of Li used represent probabilities of finding 50% of beam intensity relative to the peak. The v and Θ are laboratory velocity and scattering angle, while u and θ are c.m. quantities.

The angular distributions recorded at m/e 7 for four collision energies are shown in Fig. 3 for Li + HF and Fig. 4 for Li + HCl. The "hump" in the data near the direction of the velocity of center-of-mass of the system is due to fragmentation of reactively scattered LiX in the ionizer. The other dominating feature is the nonreactive scattering of Li at small angles. Some rainbow structure can be seen in the nonreactive data at low collision energies. The solid lines represent a fit to the nonreactive data, described in Sect. IV.C.

The laboratory angular distributions $N(\Theta)$ of LiF are shown in Fig. 5 for the four E_C. The two highest E_C distributions are at m/e 26, while the lower E_C $N(\Theta)$ are from m/e 7 measurements obtained

from the "hump" in Fig. 3 by subtracting the contribution of an assumed smooth variation in the nonreactive scattering angular distribution. Comparisons of reactive $N(\Theta)$ for the other systems obtained by this subtraction method with direct m/e 26,42 measurements show this is a reliable means for obtaining the low signal $N(\Theta)$. The data are the circles with representative error bars of ±2 standard deviation of the mean (~95% confidence limit) while the solid lines are fits to the data discussed in Sect. IV.B. The nominal Newton diagrams are shown and arrows mark the beam and c.m. positions. The low E_C data show a bimodal structure indicating formation of a complex living comparable to or longer than a rotational period, with a slight preference for scattering in the backward direction with respect to Li motion. This disappears at higher E_C where the distribution shows a weighting toward the forward direction. Figure 6 is the similar figure for the $N(\Theta)$ of LiCl recorded at m/e 42. These distributions show forward scattering of LiCl.

The TOF results at different E_C and Θ for LiF and LiCl are displayed in Figs. 7,8,9 and 10. The data shown are for m/e 7 except for one angle shown in Fig. 7, $\Theta = 40°$, where m/e 26 was measured, but the channel numbers are adjusted for the differences in the flight times. The TOF of LiCl at E_C = 9.2 kcal/mole were recorded also at m/e 42 which agreed with m/e 7 data. Again, the data are solid circles with representative error bars while solid lines are the fits to the data discussed in Sect. IV.B. Data in Fig. 9 were obtained by the single shot time-of-flight method with 2 μsec channel width. Figures 7,8, and 10 used 12 μsec channel widths characteristic of the cross correlation wheel. A

test comparison of the two techniques for LiCl at E_C = 9.2 kcal/mole showed good agreement. The time scale represented by channel numbers also contains the ion flight time of Li^+ from the ionizer through the quadrupole mass spectrometer to the scintillation type ion counter. The velocity scale shown has been corrected for this ion flight time and thus corresponds to the actual velocity of the LiCl (LiF) product.

IV. ANALYSIS OF EXPERIMENTAL RESULTS

A. Reactive Scattering: Center-of-Mass Angular and Velocity Distributions.

Two methods are used for the derivation of c.m. angular and velocity distributions of reaction products from the laboratory angular distributions and time-of-flight measurements of velocity distributions. The direct deconvolution of experimental results developed by Siska[37] based on the iterative ratio method is quite convenient, but it is also very sensitive to the noise in the data. Only for the results of Li + HCl → LiCl + H at E_c = 9.2 kcal/mole, which represent the best data in this series of experiments, was the direct deconvolution found to be successful. For most of the data, we have relied on the forward convolution to find the range of the best fit center-of-mass distributions which give good agreement with the experimental results

1. Li + HF → LiF + H.

Data for both energy systems (E_c = 3.0 and 8.7 kcal/mole) have been analyzed by using a forward convolution trial and error fitting technique in which the c.m. angular and energy distributions are input as trial functions. The corresponding laboratory angular and TOF distributions are then calculated and compared to the experimental data. The experimental resolution broadening, due to the TOF wheel and detector slit sizes, wheel velocity and ionizer length and spread in beam velocities, is taken into account. The original trial function is adjusted and the process repeated until a satisfactory fit is obtained to both

the TOF spectra and the angular distributions. The appropriate equations and basic methodology of forward convolution have been well discussed elsewhere.[38]

The c.m. product distribution is assumed to be separable into the product of a translational energy and angular part.

$$I_{c.m.}(\theta, E_T') = P(E_T')\ T(\theta). \qquad (1)$$

Although $P(E_T')$ could depend on the detailed distribution of E_C for a given nominal E_C,[39] dependence of $P(E_T')$ on E_C distribution has been neglected for these systems due to the relatively narrow beam velocity distributions, and slight sensitivity to trial calculations assuming the converse. Coupling between the energy and angular distributions is expected to occur for some reactions, but is often difficult to detect. For reactions which proceed through a long-lived complex the coupling is not important. For the systems under study the uncoupled approximation appears to be satisfactory.

The best fit calculations to the experimental angular and TOF distributions are shown as solid lines in Figs. 5 and 7 and Figs. 5 and 8 at E_C = 8.7 and 3.0 kcal/mole, respectively. Figures 11 and 12 show the resultant $T(\theta)$ and $P(E_T')$. The final result of the data fitting analysis is a c.m. contour map of product flux as a function of angle and product recoil energy. After a straightforward transformation to convert the flux distribution from an energy space to a velocity space, the c.m. contour map $I_{c.m.}(\theta,u)$ is represented in the usual form superimposed on the Newton diagram. The results are shown in Figs. 13 and 14.

In this analysis the slight energy dependence of the reactive cross section was accounted for. The absolute integral reactive cross section, σ_R, has been estimated to be 0.80 $\AA^2$ and 0.94 $\AA^2$ at E_C = 3.0 and E_C = 8.7 kcal/mole, respectively (see Sect. IV.C). A linear energy dependence has been assumed and used in fitting the two systems.

The transformation of the c.m. flux, $I_{c.m.}(\theta,u)$, to laboratory number density $N(\theta,v)$, is given by the equation[40]

$$N(\theta,v) = \frac{v}{u^2} I_{c.m.}(\theta,u)$$

The effect of the Jacobian $\frac{v}{u^2}$ for the coordinate transformation is seen in the strong enhancement of the low energy product. While the product flux actually peaks fairly well removed from the center-of-mass vector on the relative velocity axis, as seen in Figs. 13 and 14, the observed laboratory signal, which is proportional to $N(\theta,v)$, falls off rapidly away from the c.m. angle.

The fits to the laboratory angular distributions are quite good at both energies. At E_C = 8.7 kcal/mole a good fit to the TOF data is also obtained (Fig. 7). Here the peak at high velocity at each angle is due to Li nonreactivity scattered from HF. At θ = 40° this peak is not present since LiF^+ has been detected at this angle. The nonreactive peak is barely distinguishable at E_C = 3.0 kcal/mole, because of the low signal intensity and consequent noisy data (Fig. 8). Because of the uncertainties of the data at this lowest collision energy

the fit to the reactive product TOF has been only to reproduce the peak position. The sensitivity of the TOF data to the best c.m. distribution functions is low at both collision energies, but especially at the lowest one. The calculated TOF distributions vary negligibly within the uncertainty limits shown in Fig. 12 for the c.m. functions at E_C = 3.0 kcal/mole. Because the sensitivity of the laboratory angular distribution $N(\Theta)$ to $P(E_T')$ and $T(\theta)$ is strong (partly because the data obtained is higher quality) the low quality of the TOF data at this energy does not represent a significant drawback in the analysis process.

In Figs. 10a and 11a the arrows indicate the total available energy, E_{TOT}, defined by $E_{TOT} = E_C + \Delta H$, where E_C and ΔH are the canonical collision energy and reaction exoergicity, respectively. For the reaction Li + HF → LiF + H, $\Delta H = -1.1 \pm 2$ kcal/mole.[41] Shown on the same figures is also the upper limit of the total energy available E_{TOT}^{MAX}, defined as $E_{TOT}^{MAX} = E_C^{MAX} + \Delta H^{MAX}$, where E_C^{MAX} is the collision energy corresponding to the largest Newton diagram (3% of the canonical) (see for instance Fig. 2) and ΔH^{MAX} is the upper bound of the exoergicity ($\Delta H^{MAX} = -3.1$ kcal/mole). The shaded zones in Figs. 11 and 12 represent the limits for c.m. functions which give reasonable fits to the data.

The following comments are appropriate regarding Figs. 11 and 12. The c.m. angular distribution $T(\theta)$ at E_C = 3.0 kcal/mole is not quite symmetric. A slightly higher intensity appears in the backward hemisphere. A symmetric (around $\theta = 90°$) $T(\theta)$ curve gives a calculated

$N(\theta)$ too high at $\theta < \theta_{c.m.}$. The data and best fit are shown in Fig. 5. The relative intensity of $T(\theta)$ in the forward and backward hemisphere is confined within a very narrow range; decreasing or increasing $T(\theta)$ in a symmetrical manner about $\theta \approx 90°$, within the indicated dashed lines (Fig. 12b), does not signficantly affect the fit. This moderate insensitivity is due to the kinematic constraint, finite beam velocity spreads, and small amount of available energy. This explains also the low sensitivity of the TOF data to $T(\theta)$. Making the upper dashed $T(\theta)$ shallower (Fig. 12b) cancels the double peak feature in the calculated $N(\theta)$. Making the lower dashed $T(\theta)$ deeper produces the opposite effect, namely a more pronounced bimodality in the $N(\theta)$ with a simultaneous slight broadening of the entire angular disribution. The c.m. angular distribution of E_C = 8.7 kcal/mole (Fig. 11b) indicates that a large amount of product is appearing in the forward direction, but a significant amount (~33%) is still present in the backward hemisphere.

The translational energy distributions, $P(E_T')$, peak at approximately the same value (~2 to 3 kcal/mole) at the two collision energies (Figs. 11a and 12a). But the distributions peak at approximately 20% and 60% of the total available energy E_{TOT} at E_C = 8.7 and 3.0 kcal/mole, respectively. These recoil energy distributions do show a clear change as the collision energy is increased. At E_C = 3.0 kcal/mole the $P(E_T')$ rises smoothly from zero to its maximum at ~2.5 kcal/mole, then falls off rather rapidly. The fit is not too sensitive to a simultaneous

variation of the low and high E' tail of $P(E_T')$ symmetrically (Fig. 12 b), similar to $T(\theta)$. But the low or high E_T' tail can be varied independently only within a small range (<20% of the shaded area) without producing a poor fit. At E_C = 8.7 kcal/mole the $P(E_T')$ appears broader, rising from ~0.8 at ~0 kcal/mole to 1.0 at ~2 kcal/mole and then falling off not as rapidly as for E_C = 3.0 kcal/mole.

The average product translational energy,

$$\langle E_T' \rangle = \frac{\sum_{E_T'} P(E_T') \cdot E_T'}{\sum_{E_T'} P(E_T')} \qquad (2)$$

is, however, ~55% of the total available energy E_{TOT} for both collision energies.

2. Li + HCl → LiCl + H.

The best fit calculations to the experimental angular and TOF distributions are shown as solid lines in Figs. 6 and 9 and in Figs. 6 and 10 at E_C = 9.2 and E_C = 2.9 kcal/mole, respectively. The $T(\theta)$ and $P(E_T')$ which give the best fit to the data, are reported in Figs. 15 and 16. The contour maps of product flux, $I_{c.m.}(\theta,u)$, generated from these $T(\theta)$ and $P(E_T')$, are shown in Figs. 17 and 18. Since the absolute integral reactive cross section σ_R has been estimated to be 27 Å^2 and 42 Å^2 for this reaction at E_C = 2.9 and E_C = 9.2 kcal/mole, respectively (see Sect. IV-C), the substantial dependence of the reactivity upon the collision energy was taken into account in the best fit analysis, in an assumed linear form. This energy weighting makes the most probable Newton diagram for reaction somewhat larger (~6%) than the nominal most probable Newton diagram which is obtained by maximizing the quantity

$$f_i = n(v_1) \cdot n(v_2) \cdot f(\gamma) \cdot (v_1^2 + v_2^2)^{1/2}$$

where f_i is the weighting factor for the i^{th} Newton diagram. The $n(v_1)$ and $n(v_2)$ are the number density velocity distribution functions of the two reactant beams and $f(\gamma)$ is the distribution function for intersection angle γ and $(v_1^2 + v_2^2)^{1/2}$ is of course the relative velocity of the two reactants (for $\gamma = 90°$). The cross section weighting also makes the most probable collision energy somewhat larger (~12%) than the nominal collision energy, which is shown in Figs. 6,9,15, and 17, for E_C = 9.2 kcal/mole. At E_C = 2.9 kcal/mole this effect was negligible.

The fit to the experimental data is considered particularly good at the highest energy (see Figs. 6 and 9). The high quality of the data results in fairly small error bars in the best c.m. distribution functions determined. The shaded zones in Figs. 15a and 15b again represent the limits for $P(E_T')$ and $T(\theta)$ which still give a reasonable, although poorer, fit to the data. The $P(E_T')$ appears very broad, extending to the thermodynamic limit. For the reaction Li + HCl → LiCl + H, $\Delta H = -11.3 \pm 3$ kcal/mole.[41] The $T(\theta)$ is quite anisotropic and peaks at ~40°-50° in the forward direction for E_C = 9.2 kcal/mole. This feature is particularly interesting, since $T(\theta)$ reflects some characteristics of the PES which governs the reaction (see Sect. V). The sideways peaking of the product angular distribution with respect to the incident Li atom

can be more clearly seen in the c.m. contour map (Fig. 17). A similar result was obtained by direct inversion of the data as discussed later in this section (Fig. 19).

The fit to the low energy data (E_C = 2.9 kcal/mole) is not quite as good as for the high energy case. It has not been possible to improve the fit to $N(\Theta)$ (Fig. 6) without making the fit to the TOF data (Fig. 10) somewhat poorer. Nevertheless it is considered satisfactory since the reaction seems to proceed with the same mechanism for both E_C = 9.2 and 2.9 kcal/mole. In fact the best fit $P(E_T')$ (Fig. 16a) appears very similar to the one obtained for the high energy case - namely it is very broad and extends to the thermodynamic limit. The $T(\theta)$ (Fig. 16b) also is very similar, being within the indicated error bars of the high energy $T(\theta)$ (Fig. 15b). Because of the lower quality of the data and the poorer fit, no error bars have been determined for this system.

A much higher sensitivity of the TOF data to the c.m. functions is observed for HCl than HF because the Li + HCl → LiCl + H reaction is much more exoergic and a larger amount of available energy appears in translation even though the LiCl product is heavier than LiF. The $P(E_T')$ distributions peak at approximately the same value (~60%) of E_{TOT}^{MAX} (~80% of E_{TOT}) at both collision energies. The average product translational energy (Eq. (2)) is ~50% of E_{TOT}^{MAX} (~70% of E_{TOT}) at both collision energies.

For the Li + HCl system we notice the negligible contribution of the elastic peak in the TOF data, recorded at m/e = 7 (Figs. 9 and 10). If present

it should have appeared around channel 45 at $\Theta = 55°$ at $E_C = 9.2$ kcal/mole and around channel 5 at $\Theta = 70°$ at $E_C = 2.9$ kcal/mole. This fact indicates a strong depletion of the elastic scattering due to the chemical reaction and will be discussed in Sect. V.

The deconvolution method developed by Siska[37] allows $I_{c.m.}(\theta,u)$ to be obtained directly from the experimental data, without any assumption about the form of the c.m. distribution. However, this method is very sensitive to the noise in the data and thus may produce spurious results in the c.m. flux contours, unless the input data is free of significant noise or subjected to extensive smoothing. This last operation can distort the data and reduce its information content and cannot be applied in general. The difficulty of direct inversion of the data with Siska's method becomes especially serious for cases where most of the product lies close to the c.m. vector, as in the systems under study. The deconvolution method could be applied successfully only to the high resolution data obtained for Li + HCl at the highest collision energy, $E_C = 9.2$ kcal/mole. From the angular distributions of LiCl shown in Fig. 6 and from the TOF velocity analysis of LiCl shown in Fig. 9, the c.m. contour map of LiCl product flux, $I_{c.m.}(\theta,u)$, has been constructed. The result is shown in Fig. 19. Smoothing of the somewhat noisy TOF spectra has been carried out. The energy dependence of the reactive cross section has been taken into account. The results shown in Fig. 19 indicate the the LiCl product is mainly scattered sideways in the forward hemisphere with respect to the incoming Li atom beam (peak around ~50°-60°). Such a feature might suggest that the PES favors a non-linear approach. This

result confirms the interesting finding obtained from the best fit analysis described above (see Fig. 17) and is discussed in Sec. V. The laboratory data calculated from the deconvoluted c.m. flux distribution reported in Fig. 19 fit very well the experimental $N(\Theta)$ and TOF data.

The lower resolution of the cross correlation TOF data and the unfavorable kinematics of these hydrogen departing reactions has not allowed reliable application of the inversion procedure for the other systems investigated.

B. Nonreactive Scattering: Spherically Averaged Interaction Potential.

The m/e = 7 angular distributions reported in Figs. 3 and 4 at four different E_C for the Li + HF and Li + HCl system, respectively, are the results of elastic, inelastic and reactive collisions between Li atoms and the hydrogen halides. The effect of reactive encounters is clearly discernible at large angles as a hump in the angular distributions; here the m/e = 7 intensity is coming from the fragmentation in the ionizer of the LiX product. In the corresponding angular range, depletion of the nonreactive signal occurs. From the analysis of these nonreactive angular distributions interaction potentials can be determined. The characteristic oscillations which appear in the differential cross section (rainbow structure) may be partially damped by the potential anisotropy , and by the extent of the reaction probability for impact parameters near the rainbow impact parameter. When these damping effects are not severe, the rainbow extrema can provide information on the spherically symmetric portion of the potential.

Since total cross section velocity dependence measurement[7] show no quenching of the glory undulations for Li + HF and only partial quenching for Li + HCl, we do not expect much quenching of the rainbow structure for Li + HF and probably little for Li + HCl.

The experimental results of Figs. 3 and 4 were analyzed by finding the best parameters for a flexible piecewise analytical potential form that would reproduce the data in a single channel scattering calculation. Two Morse functions, a switching function and the van der Waals dispersion expansion are used for the description. The reduced form of this Morse-Morse-SW-van der Waals (MMSV) function is:

$$f(x) = \frac{V_o(r)}{\varepsilon} \qquad x = \frac{r}{r_m}$$

$$f(x) = \exp(2\beta_1(1-x)) - 2\exp(\beta_1(1-x)) \qquad 0 < x \leq 1$$

$$= \exp(2\beta_2(1-x)) - 2\exp(\beta_2(1-x)) \equiv M_2(x) \qquad 1 < x < x_1$$

$$= SW(x)\cdot M_2(x) + (1-SW(x))\cdot W(x) \qquad x_1 < x < x_2$$

$$= -C_{6r}/x^6 - C_{8r}/x^8 \equiv W(x) \qquad x_2 \leq x < \infty$$

and

$$SW = \frac{1}{2}\left[\cos\left(\frac{\pi(x-x_1)}{(x_2-x_1)}\right) + 1\right] ,$$

where $C_{6r} = \frac{C_6}{(\varepsilon r_m^6)}$, and $C_{8r} = \frac{C_8}{(\varepsilon r_m^8)}$; ε and r_m are the depth and position of potential minimum. The C_n (n = 6, 8) constants of the long range potential are given by the dispersion portion, $C_{n,disp}$, plus the induction portion, $C_{n,ind}$: $C_n = C_{n,disp} + C_{n,ind}$. The van der Waals $C_{6,disp}$ constant is estimated by the Slater-Kirkwood formula[42] for effective number of electrons:

$$C_{6,disp} = \frac{3}{2} \frac{\alpha(Li) \cdot \alpha(HX)}{[\alpha(Li)/N(Li)]^{1/2} + [\alpha(HX)/N(HX)]^{1/2}}$$

where $\alpha(Li)$ and $\alpha(HX)$ are the polarizabilities of Li atom[43] and HX (X = F, Cl)[44] respectively, and N is the number of outer shell electrons [N(Li) = 1; N(HX) = 8]. The $C_{8,disp}$ constants are estimated from the $\frac{C_8}{C_6}$ ratio[45] for He (2^1S) + Ne and Ar, and $C_{6,disp}$ of the Li + HF and HCl interaction, respectively. The C_{10} term was neglected entirely due to lack of information and to small contribution. The dipole induced dipole $C_{6,ind}$ constant is estimated by the use of the Debye equation,[46] which for our case reduces to:

$$C_{6,ind} = \alpha(Li) \cdot \mu^2(HX)$$

where $\mu(HX)$ is the dipole moment of the hydrogen halide.[47] The permanent quadrupole-induced dipole induction $C_{8,ind}$ constant is estimated by:[46]

$$C_{8,ind} = \frac{3}{2} \alpha(Li) Q^2(HX)$$

where Q(HX) is the permanent quadrupole of HX.[48]

For an assumed potential function, the center-of-mass differential cross section was calculated using the Rayleigh-Faxen-Holtsmark partial wave expansion with JWKB phase shifts. It was transformed into the laboratory frame with appropriate averaging over the velocity and angular distributions of the two beams and the detector acceptance angle. The potential parameters: ε, r_m, β_1 and β_2 were varied in an attempt to match the calculated with the experimental $N(\Theta)$ at the four collision energies. The best fit potential parameters are listed in Table II for the two systems. The spherically symmetric $V_o(r)$'s are depicted in Fig. 20. Here, r is the distance between the HF c.m. and Li. Calculated $N(\Theta)$ from the derived potentials are plotted as a solid line along with the data in Figs. 3 and 4 for the Li + HF and Li + HCl system, respectively. The calculated $N(\Theta)$ are scaled to the data by a constant scaling factor which is determined by the minimization of a χ(chi)-square goodness-of-fit measure. Considering that these are simply spherically symmetric potentials, the fit to the data, for angles smaller than the angle which corresponds to the onset of the chemical reaction, is quite good. At each energy, the calculated elastic $N(\Theta)$ for angles at which chemical reaction clearly occurs are reported as a dashed line.

Some remarks on the $N(\Theta)$ are appropriate. Rainbow scattering is fully resolved for Li + HF at the two lowest collision energies and for Li + HCl at the lowest one. In contrast to previous results,[7] this indicates that the strength of the interaction is similar for the two systems. In particular, $V_o(R)$ for Li-HF has a deeper well (ε = 0.46 kcal/mole) than for Li-HCl (ε = 0.32 kcal/mole). Because rainbow

features are resolved at low E_C for these systems, the $N(\Theta)$ are sensitive to attractive parts of the potentials. Uncertainties in the ϵ and r_m parameters are obtained by systematically varying the parameters and observing when the $N(\Theta)$ fit become poor. The estimated maximum uncertainties are within $\pm 5(\pm 7)\%$ in ϵ and r_m for Li-HF (Li-HCl). Sensitivity to the repulsive walls is less than for the well region owing to the chemical reaction which depletes the wide angle $N(\Theta)$ and to the lower signal-to-noise ratio at large angle before the onset of the reaction.

C. Reactive Scattering Cross Sections: σ_R

In a crossed molecular beam study of a chemical reaction, the integral reactive scattering cross section, σ_R, can be derived either from the integration of the angular and velocity distributions of reaction products or from the estimation of the depletion of nonreactive scattering intensity at wide angle due to chemical reactions. The latter has been used quite extensively in obtained the energy dependence of σ_R in many reactions of alkali atoms with halogen containing molecules.[19] When the reaction cross section is small, however, such as in the case of Li + HF, or when the fragmentation of reaction products in the ionizer gives the same mass spectrometric signal as the nonreactively scattered signal, which is also the case in this study, the estimation of the depletion of nonreactive scattering intensity due to chemical reaction becomes impractical. The general limitations of this method have been fully discussed.[49]

We chose to estimate the σ_R by integrating the c.m. reactive flux contour map over velocities and angular distributions following the

method developed by Birely et al.[50] In this method, the extremely difficult calibration of absolute beam intensities and absolute detection sensitivities of the apparatus is avoided by comparing reactive scattering signals with small angle elastic signals and using the theoretically calculated small angle elastic signal based on van der Waals' long range interaction,[51] $V(r) = - C/r^n$, as the absolute measure. This method suffers from considerable uncertainty even if the long range interaction is exactly known. The elastic scattering angular distribution, even at relatively small angles often shows appreciable deviation from the theoretical calculation solely based on long range interaction. More reliable calibration has been obtained using the derived spherically averaged interaction potential, $V_o(r)$, for Li + HF and Li + HCl to calculate absolute differential cross sections. This calibration was carried out at laboratory angles smaller than 7°. At this angular range, the contribution of reactively scattered lithium halides to the signals of nonreactively scattered Li signals is negligible.

In this experiment, since both elastic and reactive channels are detected at m/e = 7, the transmission through the mass spectrometer and the ion counting efficiency for both channels should be identical. The relative sensitivity for detecting reactive and elastic channels will come from the difference in the ionization cross sections for Li and lithium halides, and the Li^+:LiX^+ branching ratio of the ionization of lithium halides. At 200 eV electron energy, the ionization cross

section of Li atom is known to be 1.45 $\AA^2$.[52] In the ionization of lithium halides, we have also measured that 25% and 77% of total ions produced in LiCl and LiF are Li^+. The only quantities which are not available are the ionization cross section of lithium halides at 200 eV electron energy. We take $\alpha_{MX} \approx (\alpha_{M^+} + \alpha_{X^-}) \approx \alpha_{X^-}^{eff}$ where $\alpha_{X^-}^{eff}$ is the effective polarizability ($\alpha_{X^-}^{eff}$ = 2.2 $\AA^3$ and 0.58 $\AA^3$ for X = Cl and F, respectively).[53] Noting that the relative ionization cross section of LiF as a function of electron energy, which was measured up to 70 eV,[35a] is quite similar to that of Ne,[52] we assumed that the ionization cross sections of LiF and LiCl only differ from that of Ne (0.78 $\AA^2$) and Ar (2.46 $\AA^2$)[52] at 200 eV electron energy by the ratio of their polarizabilities (0.58 $\AA^3$/0.4 $\AA^3$ and 2.2 $\AA^3$/1.6 $\AA^3$).[54] These estimated values for LiCl and LiF are 3.1 $\AA^2$ and 1.04 $\AA^2$.

With these values, we obtained reactive cross sections of 42 and 27 $\AA^2$ for Li + HCl → LiCl + H at collision energies of 9.2 and 2.9 kcal/mole, respectively, and 0.94 and 0.8 $\AA^2$ for Li + HF → LiF + H at collision energies of 8.7 and 3.0 kcal/mole. The largest uncertainties of these estimates of σ_R probably come from the estimation of ionization cross sections of lithium halides and the spherically averaged interaction potential. Nevertheless, the absolute value of reactive cross sections obtained in these experiments, should be accurate within a factor of 2 and the relative values for the two systems and at different collision energies are estimated to be accurate to within 30%.

V. DISCUSSION

The derived maps of product flux in the c.m. frame allow an evaluation of the dynamical influence of the PES as well as the kinematic constraints for these two reactions. Some inferences are clear while others are intended to suggest possibilities and stimulate dynamical calculations, as well as new calculations of the potential energy surface for LiClH. A detailed description and discussion of the potential energy surface of LiFH have been given recently by Chen and Schaefer.[6]

A. Li + HF → LiF + H.

1. Product Energy Distributions.

A dominant feature of this reaction is the large fraction of available energy released into translation. The $P(E_T')$ distributions derived are shown in Figs. 11a and 12a, where for both of these E_C the average product translational energy is ~55% of E_{TOT}. The PES of Chen and Schaefer[6] shows a late barrier to reaction, a form of repulsive energy release, and classical trajectory studies[55,56] have shown this feature to result in large amounts of energy in translation, in agreement with these findings.

For the collision energy, E_C = 3.0 kcal/mole, the remaining ~45% of E_{TOT} is predominantly in the rotational excitation of the ground vibrational state because the amount of average internal excitation in LiF shown in Fig. 12a is not quite sufficient to populate LiF(v=1) which contains 2.6 kcal/mole of vibrational energy. Trajectory studies

have suggested[55,56] that for this mass combination the energy release in the vibrational and translational degrees of freedom will be "mixed" due to "cutting the corner" of the PES rather than going strongly to E_T' for a repulsive PES: but this is not found here. However, H atom tunneling through a very high late barrier rather than simply exoergic late energy release, and a non-LEPS-type surface are deviations from the previous trajectory studies and make the generalized conclusions tenuous.[57,58]

At E_C = 8.7 kcal/mole the possibility of a greater role for vibrational excitation of LiF cannot be ruled out due to the broad nature of the $P(E_T')$ (see Fig. 11a). The general trend from trajectory studies and experiment[55,56,59,60] of increasing E_C being channeled to product translational and rotational (E_R') cannot be tested due to lack of knowledge of $P(E_R')$. A significant increase in $\langle E_T' \rangle$ is observed however in support of this trend, though the peak position in $P(E_T')$ is not changing here with E_C. For a light particle leaving a heavy atom, the potential energy of the exit barrier is likely to channel into product translation. The fact that the product translational energy peaks at 3 kcal/mole at both collision energies might be a tunneling phenomenon or may indicate that the exit channel barrier is significantly less than the estimate of 6 kcal/mole by Chen and Schaefer.[6]

2. Angular Distributions.

The $T(\theta)$ in Fig. 12b for E_C = 3.0 kcal/mole contains a significant amount of information. While this $T(\theta)$ is slightly backward peaked with respect to the Li direction, it is, to a good approximation, symmetric about $\theta = 90°$, and the following remarks focus on this feature.

Though this symmetry in principle is possible in a direct interaction, it is very likely the result of the formation of a Li-F-H complex with a lifetime comparable to or longer than its rotational period. At this relatively low E_C, this is not surprising due to the known complex stability, calculated[2,6] to be about 4 kcal/mole with respect to the Li and HF reactants. The minimum in $T(\theta)$ is less than 1/2 of the values at the poles (0° and 180°). This strong peaking at the poles is somewhat surprising for a system which produces a light hydrogen atom and heavier LiF, since most of the initial angular momentum is expected to appear as rotational angular momentum of LiF, and the final orbital angular momentum is not expected to be strongly correlated to the initial orbital angular momentum. From the observation of this type of $T(\theta)$ we can conclude[61,62] that there is a strong preference for hydrogen emission in the plane which is perpendicular to the initial orbital angular momentum, such that the final orbital angular momentum is nearly parallel or antiparallel to the initial orbital angular momentum. This strong correlation of initial and final orbital angular momentum can occur if the reactions are mainly due to a coplanar encounter of atoms and molecules.

To appreciate how the significant coplanarity of the reaction is a dynamical effect, consider the kinematic and statistical predictions for the LiFH system. Due to the extremely low final reduced mass μ' and a reasonable range of exit impact parameters b', it is apparent that $|\vec{L}'| << |\vec{L}|$ where $\vec{L}$ is the orbital angular momentum vector of reactants. With low rotational J values for the HF beam, we have

the kinematic constraint $\vec{J}' \approx \vec{L}$. The small $\vec{L}'$ is predicted to be $\simeq \vec{J}$ by both the classical mechanical spectator stripping model[63] and quantum and classical mechanical theories of angular momentum coupling in reactions.[14] Some phase space calculations[64] make similar predictions, although it does not appear to be a general conclusion.[65] Given an isotropic initial $\vec{J}$ distribution, this predicts an isotropic $\vec{L}'$, not confined perpendicular to the initial scattering plane, resulting in an isotropic $I_{c.m.}(\theta,E_T')$.[66] The results of Fig. 12b support the conclusion of coplanar encounter for this system such that the strong correlation between $\vec{L}$ and $\vec{J}$ causes the orientation of $\vec{L}'$ to be mostly parallel or antiparallel to $\vec{L}$, and not isotropically oriented.

If there is a force which brings the H atom into the plane determined by the relative motion between Li and F atoms during the course of reaction, the strong correlation between $\vec{L}$ and $\vec{L}'$ will not be the consequence of the correlation between $\vec{L}$ and $\vec{J}$, but the PES of Chen and Schaefer[6] does not show any strong forces to bring H into the plane determined by the relative motion between Li and F atoms for initially out of plane conditions. This means that for the reaction to occur the motion of the H atom itself must also lie in the same plane determined by the relative motion between Li and F and thus a small opacity will result. The possible important role of some substantially rotationally excited HF in the beam is relevent here. Because, not all of the HF in the supersonic beam may relax, particularly since the oven temperature is high enough to thermally populate HF with a relatively high rotational quantum number with large level spacings. A bimodal distribution in J for HF might result after a weak expansion through the nozzle. If the

contribution from the HF in higher J is important, the observed coplanarity means that $\vec{J}$ and $\vec{L}$ must be parallel or antiparallel, suggesting that rotation might be efficient in surmounting or tunneling through the exit barrier.

At E_C = 3.0 kcal/mole Fig. 12b also shows a slight backward peaking of the product. Perhaps at this E_C some backward scattered collisions are those such that Li approaches F as H rotates into Li, exciting the bending of the complex and leading to the formation of products after passing through the exit barrier. The calculated transition state of LiFH is bent at 74°.[6] For such a collision $\vec{J}$ and $\vec{L}$ are likely to be antiparallel; $\vec{J}'$ and $\vec{L}'$, and $\vec{L}$ and $\vec{L}'$ are parallel.

It should be noted that trajectory studies on a late barrier surface,[56] for all mass combinations, show a tendency toward backward scattering, in agreement with this observation at E_C = 3.0 kcal/mole. These trajectory studies however employ LEPS-type surfaces where collinear approach is favored, unlike the predicted[6] bent transition state.

Figure 11b shows forward scattering at E_C = 8.7 kcal/mole, in contrast to Fig. 12b. At this higher E_C the formation of a long lived complex should not be important. This forward scattering at higher collision energy is fairly consistent with Roach's direct interaction model[67] for Chen and Schaefer's transition state.[6] In this model, reaction occurs if (a) there is sufficient E_C to reach the "corner" of the PES and (b) the vibrational energy is

larger than the difference between the top of the potential barrier and the corner energy. The scattering angle, θ, is predicted from the reacting geometry alone considering the light H motion to be decoupled from the heavier LiF motion; $\theta = \varepsilon$, the angle between the initial relative velocity and the F-H bond axis. The transition state Li-F-H angle[6] of 74° predicts somewhat forward scattering for the model. This agreement with Roach's model here could also be fortuitous.

At E_C = 3.0 kcal/mole, because the observed $P(E_T')$ (Fig. 12a) shows that vibrational excitation of LiF generally will not be energetically possible, we have $E_R' = E_{TOT} - E_T'$. The average $\langle E_R' \rangle \simeq 1.8$ kcal/mole, or $\langle J' \rangle \simeq 20\hbar$. The calculated transition state[6] can be used to get an estimate of b' and thus L'. Assuming H atom pushes off directly from F, then b' $\cong$ 0.44 Å, and for $\langle E_T' \rangle$ = 2.3 kcal/mole we have $\langle L' \rangle \simeq 3\hbar$. The domination of $\langle J' \rangle$ over $\langle L' \rangle$ is just what would be expected for this system. The maximum values are $J'_{MAX} \simeq 32\hbar$ and $L'_{MAX} \simeq 4\hbar$. But because the initial orbital angular momentum must be carried away as rotational motion of LiF, it is not possible to have all the available energy carried away as translation. Because of the broader $P(E_T')$ for E_C = 8.7 kcal/mole, $\langle E_R' \rangle$ cannot be estimated; however the maximum possible $E_R'(=E_{TOT})$ would give $J' \simeq 50\hbar$, and $E_T' = E_{TOT}$ would give $L' = 6\hbar$ using b' = 0.44 Å. It is worth noting that although L' is constrained to be small $\langle E_T' \rangle$ can be large for a system with small μ'.

3. Integral Cross Sections and Potential Energy Barrier.

From the kinematic constraint $\vec{L} \simeq \vec{J}'$, for E_C = 3.0 kcal/mole, $L_{MAX} \simeq 32\hbar$ corresponds to a b_{MAX} = 1.8 Å. And for $\sigma_R \simeq 0.80$ Å^2 this

gives an average opacity of 0.08, a rather low value. At E_C = 8.7 kcal/mole, taking $L_{MAX} \simeq 50\hbar$ yields $b_{MAX} \simeq 1.6$ Å. With $\sigma_R \simeq 0.94$ Å^2, this gives an average opacity of 0.12. The relatively small average opacity probably reflects the restricted orientation requirement discussed above, as well as the existence of a barrier and a tight geometrical requirement about the transition state geometry.[6] The energy dependence of σ_R is not a simple function, at least in phase space theory,[68] but depends on the product of the probability of "complex" formation and the probability of the "complex" decomposing to products. The size of these two factors likely have opposite behavior with E_C and a fairly constant σ_R, at least over this limited range of collision energies, is not surprising.

The slight dependence on E_C of σ_R for this PES[6] with a barrier in the exit channel is also consistent with trajectory studies.[55,56] These show reagent vibration as efficient in promoting reaction and reagent translation inefficient.

It is tempting to try to assign a maximum barrier height based on the observation of products at the nominal E_C = 2.2 kcal/mole, with the possible contribution of high energy parts of the beam distributions. However, given the relatively small size of the observed σ_R and results of tunneling studies[69] it would be imprudent to try to make such an assignment. Recent calculations[6] show a barrier, with zero-point energies, of about 6 kcal/mole. If this value is accurate, all the products of LiF formed at the nominal E_C = 2.2 kcal/mole are through tunneling.

B. $Li + HCl \rightarrow LiCl + H$.

Product energy in translation dominates in this reaction, with $\langle E_T' \rangle \simeq 70\%$ of E_{TOT} for both $E_C = 2.9$ and 9.2 kcal/mole (see Figs. 15a and 16a). The $P(E_T')$ are very broad and both peak at ~80% of E_{TOT}. A significant barrier ($\gtrsim 2$ kcal/mole) likely does not exist due to the large σ_R at low E_C. For this exoergic reaction a late energy release (repulsive) surface would probably give accord of experimental observations with trajectory studies.[55,56] This is in opposition to the previously calculated semiempirical PES[5] which shows a substantial barrier in the entrance channel.

Unfortunately, no information can be gained from the data as to the relative importance of product E_R' and E_V' by direct measurement. However, by consideration of the size of σ_R we may reach a conclusion regarding the internal degrees of freedom of nascent LiCl. At E_C = 9.2 kcal/mole, $\sigma_R \simeq 42$ Å^2, and assuming an opacity of unity, b_{MAX} = 3.66 Å or $L_{MAX} \simeq 120\hbar$. Due to the light departing H we again have the kinematic constraint $\vec{L} \simeq \vec{J}'$, leading to E_R' = 29 kcal/mole which corresponds to E_{TOT}^{MAX} for L_{MAX}. That is, L_{MAX} cannot be larger than $120\hbar$ and so the opacity function f(b) is to a good approximation a step function:[70]

$$f(b) = 1 \qquad b \leq b_{MAX} \tag{3}$$

$$= 0 \qquad b > b_{MAX}.$$

Because

$$\sigma_R = 2\pi \int_0^\infty f(b)\, b\, db \tag{4}$$

$$\text{and} \qquad P(b) = 2\pi b f(b)/\sigma_R \tag{5}$$

where P(b) is the probability distribution for reaction occuring between b and b + db as well as classically,

$$P(b)db = P(L)dL \simeq P(J')dJ' \tag{6}$$

$$\text{and} \qquad P(E_R') = P(J')\frac{dJ'}{dE_R'} \propto P(J')/J' \propto P(b)/b \tag{7}$$

$$\text{then} \qquad P(E_R') \propto 2\pi b f(b)/(\sigma_R b) \propto 2\pi f(b)/\sigma_R \propto \text{constant}. \tag{8}$$

The range of E_R' will be between 0 and E_{TOT}^{MAX}. The measured $P(E_T')$ of Fig. 15a is, to a first approximation, so broad as to be constant. Taking the product $P(E_T')P(E_R')$ to be constant over the entire energy range, with average energy of approximately 50% of E_{TOT}^{MAX}, restricts the combined distribution $P(E_T',E_R') = P(E_T',E_R',E_V')$ to a contour along $E_V' = 0$. Thus for this system the conclusion is that, approximately, very little energy should appear in vibrational excitation at higher collision energy. Assuming a unit opacity for reaction at E_C = 2.9 kcal/mole gives $L_{MAX} \simeq J'_{MAX} = 55\hbar$ and E_R' quite short of E_{TOT} as well as E_{TOT}^{MAX}. Thus at the lower E_C the arguments above regarding $P(E_R')$ etc. cannot be made.

The large amount of product energy in translation, negligible barrier, rather large σ_R, and mass combination bears similarity to the recent work by Gupta, et al.[59] on Ba + HF. In that study it was suggested that the governing PES had very late downhill energy release. Furthermore, the energy release being further in the exit channel than

common for exoergic reactions would make "cutting the corner" for "mixed" energy release unimportant. These conclusions seem to apply to Li + HCl also. At higher collision energy, the increased translational energy for Li + HCl is going over to product translation and rotation also similar to that found for BaF[59] (at least at the upper range of their E_C), and suggested by earlier work.[55,56,60]

The σ_R for both LiCl and LiF formation appear roughly independent of E_C but differ considerably in magnitude. The dramatic size difference correlates well with the differences in vertical electron affinity (V.E.A.)[71] as well as exoergicity. For $HX + e^- \rightarrow HX^-$ the V.E.A. are about +4 eV for HF and +1 eV for HCl. Therefore no ionic-covalent curve crossing is possible for either system outside the van der Waals radii.[27] Yet for LiCl formation, at least at E_C = 9.2 kcal/mole, σ_R seems to be limited by only the conservation laws. This says that nearly all HCl orientations will react which is a bit surprising given that the harpooning mechanism is not an appropriate description.

Figures 15b, 16b, 17, 18 and 19 display the angular distributions of the LiCl product. The $T(\theta)$ are strongly forward peaked. At E_C = 9.2 kcal/mole it is clear that $T(\theta)$ peaks at $\theta \simeq 40° - 50°$, while the exact peak location at E_C = 2.9 kcal/mole is uncertain. These results are not easily explained except the obvious conclusion of not forming long lived complexes in this reaction.

No information has been obtained in the present work on the spatial correlation between the $\vec{L}$ and $\vec{L}'$, but no strong correlation

is expected in this case since the large cross section indicates no geometric constraint in the entrance channel. From the large σ_R and the kinematic constraint $\vec{L} \simeq \vec{J}'$ large values of product rotation have been derived. Again, the small μ' means $\vec{L}'$ must be relatively small showing that, as for LiF, large fractions of the total energy available can appear in translation while L' is small and J' rather large.

C. Spherically Averaged Interaction Potential: $V_o(r)$.

We conclude this discussion with a few comments about the spherically symmetric potential $V_o(r)$ determinations, or more precisely, the physical significance of fitting a $V_o(r)$ by single channel scattering techniques to the nonreactive Li + HX scattering. For the similar non-reactive atom-diatom case (e.g., rare gas + HX), it has been shown[72] that only under favorable conditions can an accurate spherically averaged potential be extracted. Also, for simple systems like rare gas + HX the full anisotropic potential cannot be derived with confidence from only a total (elastic plus inelastic) differential cross section measurement. In the present study the HF beam characteristics were the same as used in the HF + Xe study[72] where it was argued that the $V_o(r)$ extraction was valid due to the likely significant population of $J \geq 1$, in the HF beam, the small rotational excitation cross section due to a large rotational constant for HF and the ability to fit the structured $N(\Theta)$ at more than one E_C. These same arguments also apply in Li + HX systems described in this paper. Also estimates of b_{MAX} from σ_R for Li + HCl indicate little reactive scattering for $b \gtrsim 3.5$ Å, and only moderate quenching of glory oscillations was observed[7] for integral

cross section measurements of Li off HCl. Very little glory quenching for Li + HF[7] and the small reactive σ_R for LiF formation suggest reaction is not significantly obscuring nonreactive scattering events with moderate b values. On the other hand, the degree of the anisotropy for the interaction may be great enough as to negate comparisons to the HF + Xe study.[72] Together with the still unknown complicating feature of reaction, we suggest that although the derived $V_o(r)$ of Fig. 20 might not give an exact picture, it is of definite qualitative value. Furthermore, attractive well determination is generally more reliable from only a series of $N(\Theta)$ at different E_C showing rainbow structure than from only nonreactive integral cross section measurements. Also, the glory impact parameter is smaller (more likely reactive) than for rainbow scattering. These facts suggest the present $V_o(r)$ results may be preferable to previous $V_o(r)$ results[7] and related anisotropy evaluations.[73]

ACKNOWLEDGEMENTS

The authors gratefully acknowledge many useful discussions with R.J. Buss, K. Shobatake, M. Chen, and H.F. Schaefer. C.H.B. thanks also Professor James L. Kinsey for a helpful and stimulating discussion. This work was supported by the Division of Chemical Sciences, Office of Basic Energy Sciences, U.S. Department of Energy under contract W-7405-Eng-48. P.C. acknowledges a fellowship from the Italian National Research Council (CNR) during the early stages of this work and a fellowship from the Italian Ministry of Education and travel support from NATO grant No. 1444 during the final stages. P.W.T. acknowledges a fellowship from the Fundagas de Amparo a Pesquiso do Estado de Sao Paulo.

REFERENCES

1. W. A. Lester, Jr. and M. Krauss, J. Chem. Phys. 52, 4775 (1970); W. A. Lester, Jr. ibid. 53, 1611 (1970).
2. M. Trenary, H. F. Schaefer, J. Chem. Phys. 68, 4047 (1978).
3. G. G. Balint-Kurti and R. N. Yardley, Faraday Disc. Chem. Soc. 62, 77 (1977).
4. Y. Zeiri and M. Shapiro, Chem. Phys. 31, 217 (1978).
5. M. Shapiro and Y. Zeiri, J. Chem. Phys. 70, 5264 (1979).
6. M. M. L. Chen and H. F. Schaefer III, J. Chem. Phys., in press.
7. R. K. B. Helbing and E. W. Rothe, J. Chem. Phys. 48, 3945 (1968).
8. J. N. L. Connor, Comp. Phys. Comm. 17, 117 (1979).
9. Atom-molecule Collision Theory, ed. R. B. Bernstein, (Plenum, New York, 1979).
10. M. R. Levy, Prog. React. Kin. 10, No. 1-2 (1979).
11. C. L. Vila, D. J. Zvijac, and J. Ross, J. Chem. Phys. 70, 5362 (1979).
12. V. Khare, D. J. Kouri, and M. Baer, J. Chem. Phys. 71, 1188 (1979).
13. J. C. Light and A. Altenberger-Siezek, J. Chem. Phys. 64, 1907 (1976).
14. K. Schulten and R. G. Gordon, J. Chem. Phys. 64, 2918 (1976); see also G. Venzl and S. F. Fischer, J. Chem. Phys. 71, 4175 (1979).
15. E. H. Taylor and S. Datz, J. Chem. Phys. 23, 1711 (1955).
16. D. R. Herschbach, J. Chem. Phys. 33, 1870 (1960).
17. S. Datz, D. R. Herschbach and E. H. Taylor, J. Chem. Phys. 35, 1549 (1961).

18. K. T. Gillen, C. Riley and R. B. Bernstein, J.Chem. Phys. 50, 4019 (1969).

19. E. F. Greene, A. L. Moursund and J. Ross, Adv. Chem. Phys. 10, 135 (1966).

20. J. R. Airey, E. F. Greene, K. Kodera, G. P. Peck and J. Ross, J. Chem. Phys. 46, 3287 (1967); and earlier references cited therein.

21. L. R. Martin and J. L. Kinsey, J. Chem. Phys. 46, 4834 (1967).

22. (a) T. J. Odiorne and P. R. Brooks, J. Chem. Phys. 51, 4676 (1969); (b) T. J. Odiorne, P. R. Brooks, and J. V. V. Kasper, J. Chem. Phys. 55, 1980 (1971); (c) J. G. Pruett, F. R. Grabiner and P. R. Brooks, J. Chem. Phys. 63, 1173 (1975); (d) M. W. Geis, H. H. Dispert, T. L. Budzynski and P. R. Brooks, Am. Chem. Soc. Symp. Ser. 56, 103 (1977).

23. P. E. Siska, Ph.D. Thesis, Harvard University, Cambridge, Mass., 1970.

24. D. R. Herschbach, Faraday Discuss. Chem. Soc. 62, 162 (1977).

25. R. R. Herm and D. R. Herschbach, J. Chem. Phys. 43, 2139 (1965).

26. C. Maltz and D. R. Herschbach, Faraday Discuss. Chem. Soc. 44, 176 (1967); C. Maltz, Ph.D. Thesis, Harvard University, Cambridge, Mass., 1969.

27. See: D. R. Herschbach, Adv. Chem. Phys. 10, 319 (1966).

28. H. H. Dispert, M. W. Geis and P. R. Brooks, J. Chem. Phys. 70, 5317 (1979).

29. On the effect of rotational energy on reactions, see: A. E. Proctor and R. B. Bernstein, J. Chem. Phys. 62, 2506 (1975); S. Stolte, A. E. Proctor, W. M. Pope and R. B. Bernstein, J. Chem. Phys. 66, 3468 (1977); L. Zandee and R. B. Bernstein, J. Chem. Phys. 68, 3760 (1978); F. S. Klein and A. Persky, J. Chem. Phys. 61, 2472 (1974).

30. B. A. Blackwell, J. C. Polanyi and J. J. Sloan, Faraday Discuss. Chem. Soc. 62, 147 (1977); Chem. Phys. 30, 299 (1978).

31. Y. T. Lee, J. D. McDonald, P. R. LeBreton and D. R. Herschbach, Rev. Sci. Instr. 40, 1402 (1969).

32. P. E. Siska, J. M. Parson, T. P. Schafer and Y. T. Lee, J. Chem. Phys. 55, 5762 (1971).

33. K. Sköld, Nucl. Instrum. Meth. 63, 114 (1968); V. L. Hirschy and J. P. Aldridge, Rev. Sci. Instr. 42, 381 (1971); J. M. Farrar, Ph.D. dissertation, University of Chicago, Chicago, Illinois, 1974; C. V. Nowikov and R. Grice, J. Phys. E: Sci. Instr. 12, 515 (1979).

34. Atlas of Mass Spectral Data, E. Stenhagen, S. Abrahamsson and F. W. McLafferty, Eds. (Interscience, New York, 1969); Vol. I.

35. (a) R. T. Grimley, J. A. Forsman and Q. G. Grindstaff, J. Phys. Chem. 82, 632 (1978); (b) P. Mohazzabi and A. W. Searcy, Int. J. Mass Spectrom. Ion Phys. 24, 469 (1977).

36. J. Berkowitz, H. A. Tasman and W. A. Chupka, J. Chem. Phys. 36, 2170 (1962).

37. P. E. Siska, J. Chem. Phys. 59, 6052 (1973).

38. J. M. Farrar, Ph.D. dissertation, University of Chicago, Chicago, Illinois, 1974. The program used is described in the Ph.D. dissertation of R. J. Buss, University of California, Berkeley, California, 1979.

39. This is particularly likely for thermoneutral or endoergic reactions in which the total energy available to the fragments can be strongly increasing with collision energy.

40. E. A. Entemann, Ph.D. dissertation, Harvard University, Cambridge, Mass., 1967; also T. T. Warnock and R. B. Bernstein, J. Chem. Phys. 49, 1878 (1968).

41. The heats of formation of LiF and LiCl are taken from S. W. Benson, Thermochemical Kinetics, (John Wiley and Sons, Inc., New York, 1968). Those of Li, HF, HCl and H from J. Phys. Chem. Ref. Data 6, Suppl. 1 (1977). The uncertainty in ΔH results from the uncertainty in the LiX bond dissociation energy, for example, see: J. Berkowitz, C. H. Batson and G. L. Goodman, J. Chem. Phys. 71, 2624 (1979).

42. J. C. Slater and J. G. Kirkwood, Phys. Rev. 37, 682 (1931); see also K. S. Pitzer, Adv. Chem. Phys. 2, 59 (1959).

43. H. J. Werner and W. Meyer, Phys. Rev. A 13, 13 (1976).

44. A. A. Maryott and F. Buckley, Natl. Bur. Std. (U.S.) Circ. No. 537 (1953).

45. C. H. Chen, H. Haberland and Y. T. Lee, J. Chem. Phys. 61, 3095 (1974).

46. J. O. Hirschfelder, C. F. Curtiss and R. B. Bird, Molecular Theory of Gases and Liquids, (Wiley, New York, 1964).

47. J. S. Muenter, J. Chem. Phys. 56, 5409 (1972).

48. D. E. Stogryn and A. D. Stogryn, Mol. Phys. 11, 371 (1966).

49. J. L. Kinsey, in MTP International Review of Science, ed. J. C. Polanyi (Butterworths, London, 1972), Vol. 9, p. 173; J. P. Toennies, in Physical Chemistry, Vol. VIA, Kinetics of Gas Reactions, Academic Press, New York (1974).

50. See for ex. J. H. Birely, R. R. Herm, K. R. Wilson and D. R. Herschbach, J. Chem. Phys. 47, 993 (1967).

51. See for ex., (a) E. A. Mason, J. T. Vanderslice and J. G. Raw, J. Chem. Phys. 40, 2153 (1964); (b) R. B. Bernstein, Adv. Chem. Phys. 10, 81 (1966).

52. S. C. Brown, Basic Data of Plasma Physics, 1966, (The MIT Press, 2nd ed., 1967), p. 143.

53. P. Brumer and M. Karplus, J. Chem. Phys. 58, 3903 (1973).

54. J. S. Cohen and R. T. Pack, J. Chem. Phys. 61, 2372 (1974).

55. P. J. Kuntz, in Dynamics of Molecular Collisions, Part B (W. H. Miller, ed.), Plenum, New York (1976).

56. J. C. Polanyi and J. L. Schreiber, in Physical Chemistry an Advanced Treatise, vol. VIA, (W. Jost, ed.), Academic Press, New York (1974).

57. Concerning the use of LEPS-type surfaces, see for example, H. Schor, S. Chapman, S. Green, and R. N. Zare, J. Chem. Phys. 69, 3790 (1978).

58. For recent tunneling studies see, e.g., J. N. L. Connor, W. Jakubetz, and J. Manz, Chem. Phys. 28, 219 (1978); J. N. L. Connor and A. Laganà, Comp. Phys. Comm. 17, 145 (1979).

59. A. Gupta, D. S. Perry, and R. N. Zare, submitted to J. Chem. Phys.

60. L. Cowley, D. S. Horne, and J. C. Polanyi, Chem. Phys. Lett. 12, 144 (1971); A. M. G. Ding, L. J. Kirsch, D. S. Perry, J. C. Polanyi, and J. L. Schreiber, Faraday Disc. Chem. Soc. 55, 252 (1973); J. C. Polanyi, J. T. Sloan and J. Wanner, Chem. Phys. 13, 1 (1976); D. S. Perry and J. C. Polanyi, Chem. Phys. 12, 419 (1976).

61. D. R. Herschbach, Faraday Disc. Chem. Soc. 33, 149 (1962).

62. W. B. Miller, S. A. Safron, and D. R. Herschbach, Faraday Disc. Chem. Soc. 44, 108 (1967); J. Chem. Phys. 56, 3581 (1972).

63. D. R. Herschbach, Appl. Opt. Suppl. 2, 128 (1965).

64. J. C. Lin and J. C. Light, J. Chem. Phys. 45, 2545 (1966); P. Pechukas, J. C. Light, and C. Rankin, J. Chem. Phys. 44, 794 (1966).

65. A slight departure from $L \approx J'$ for the K + HBr reaction is discussed in: D. A. Case and D. R. Herschbach, Mol. Phys. 30, 1537 (1975).

66. Caution must be observed when considering the average relative orientation of L' and J' because statistical calculations have shown the possibility of significant alignment in the absence of dynamical effects (D. A. Case and D. R. Herschbach, J. Chem. Phys. 64, 4212 (1976)). These calculations for systems similar to LiFH however predict negligible orientational effects.

67. A. C. Roach, Chem. Phys. Lett. 6, 389 (1970); Faraday Disc. Chem. Soc. 62, 151 (1977). See the discussion concerning Figs. 17 and 18 of Ref. 6 also.

68. J. C. Light, Faraday Disc. Chem. Soc. 44, 14 (1967).

69. W. H. Miller, J. Am. Chem. Soc. 101, 6810 (1979).

70. This is similar to that found for K + HBr. See, J. R. Airey, E. F. Greene, K. Kodera, G. P. Peck, and J. Ross, J. Chem. Phys. 46, 3287 (1967).

71. D. C. Frost and C. A McDowell, J. Chem. Phys. 29, 503 (1958).

72. C. H. Becker, P. W. Tiedemann, J. J. Valentini, Y. T. Lee, and R. B. Walker, J. Chem. Phys. 71, 481 (1979).

73. R. E. Olson and R. B. Bernstein, J. Chem. Phys. 50 246 (1969); erratum 71, 2330 (1979).

Table I. Beams Characteristics and Center-of-Mass Collision Energies.

Li Beam Carrier Gas	T/K	M	Peak $v/10^4$ cm sec^{-1}	(FWHM) $\Delta v/v$	E_C/kcal $mole^{-1}$ Li + HF	Li + HCl
He	2116	5.5	35.7	31%	8.7	9.2
85% He + 15% Ne	1475	4.7	29.8	35%	5.7	6.9
Ne	545	4.9	18.1	33%	3.0	2.9
Ar	294	5.6	13.3	31%	2.2	1.9
HF	603	8.5	13.1	22%		
HCl	620	7.2	9.9	25%		

Table II. Best fit $V_o(r)$ Potential Parameters for Li-HF and Li-HCl.

	Li - HF	Li - HCl
ε (kcal/mole)	0.46	0.32
r_m (Å)	4.34	4.7
β_1	4.0	4.6
β_2	10.0	8.0
x_1	1.0693	1.0866
x_2	1.600	1.700
C_6 (kcal/mole·Å^6)	2556.0	4541.0
C_8 (kcal/mole·Å^8)	22000.0	36800.0

FIGURE CAPTIONS

Fig. 1. Beam velocity distributions for the indicated substances under the experimental conditions, each normalized to unity. Solid circles are from TOF data and lines are results of parametric fits to the deconvoluted distributions for the Mach numbers and temperatures given in Table I.

Fig. 2. Exemplary Newton diagrams for Li + HCl at E_c = 9.2 kcal/mole. The solid relative velocity line ($\vec{v}_{Li}-\vec{v}_{HCl}$) corresponds to the most probable velocities, while dashed lines indicate the FWHM velocity spreads. The v and Θ are laboratory velocity and scattering angle, while u and θ are c.m. quantities. The circles represent the maximum energetically permitted u'_{LiCl}. Primed quantities are final values.

Fig. 3. Measured angular distributions (open circles) at m/e 7 for Li + HF at four collision energies with exemplary error bars of ±2 standard deviation of the mean. The "hump" around the indicated center-of-mass position is due to reactive scattering (see text). Solid lines are fits to the nonreactive scattering, described in Sect. IV.C.

Fig. 4. Same as Fig. 3 except for Li + HCl.

Fig. 5. Measured angular distributions of LiF product (solid circles) with error bars representing ±2 standard deviations of the mean (~95% confidence limit). Nominal Newton diagrams and beam and c.m. positions are shown for the four E_c. Low signal data are recorded at m/e = 7 (see text). Solid lines are fits to the data discussed in Sect. IV.B.

Fig. 6. Same as Fig. 5 except for LiCl product all measured at m/e = 42.

Fig. 7. Measured TOF spectra (solid circles) of LiF at E_c = 8.7 kcal/mole at different laboratory scattering angles measured at the indicated values of m/e. The cross correlation method was used. Solid lines are fits to the data discussed in Sect. IV.B. Fast peaks are nonreactively scattered Li (dashed lines are drawn through the experimental points for clarity).

Fig. 8. Same as Fig. 7 except for LiF at E_c = 3.0 kcal/mole, measured at m/e = 7.

Fig. 9. Same as Fig. 7 except for LiCl at E_c = 9.2 kcal/mole, measured at m/e = 7, and the single shot TOF method was used.

Fig. 10. Same as Fig. 7 except for LiCl at E_c = 2.9 kcal/mole, measured at m/e = 7.

Fig. 11. Best fit (a) translational energy and (b) angular distributions (solid lines) for Li + HF → LiF + H at E_c = 8.7 kcal/mole. The shaded area represents the limits of acceptable fits to the data. The exoergicity (ΔH) is shown in part (a) as is the total energy available (E_{TOT}) estimated by the sum of the recommended value of ΔH and the nominal E_c, and the maximum available energy (E_{TOT}^{MAX}) given by the sum of the upper bound estimate on $-\Delta H$ and the maximum E_c obtained from 3% values of the beam velocity spread.

Fig. 12. Same as Fig. 11 except for the nominal E_c = 3.0 kcal/mole.

Fig. 13. Center-of-mass LiF product flux contour map superimposed on the nominal Newton diagram for E_c = 8.7 kcal/mole, derived from the best fit analysis (forward convolution method).

Fig. 14. Same as in Fig. 13 except for LiF at E_c = 3.0 kcal/mole.

Fig. 15. Same as in Fig. 11 except for Li + HCl → LiCl + H at E_c = 9.2 kcal/mole.

Fig. 16. Same as in Fig. 11 except for Li + Cl → LiCl + H at E_c = 2.9 kcal/mole. Regions of distributions giving acceptable fits to the data are not estimated due to the lower quality of the data and somewhat poorer fit with respect to the 9.2 kcal/mole results.

Fig. 17. Center-of-mass LiCl product flux contour map superimposed on the nominal Newton diagram for E_c = 9.2 kcal/mole, derived from the best fit analysis (forward convolution method).

Fig. 18. Same as in Fig. 17 except for E_c = 2.9 kcal/mole.

Fig. 19. Same as Fig. 17 except derived from direct deconvolution of the $N(\Theta)$ and TOF data by Siska's ratio method.

Fig. 20. Derived spherically symmetrical interaction potentials for Li-HF and Li-HCl. Potential parameters are given in Table II.

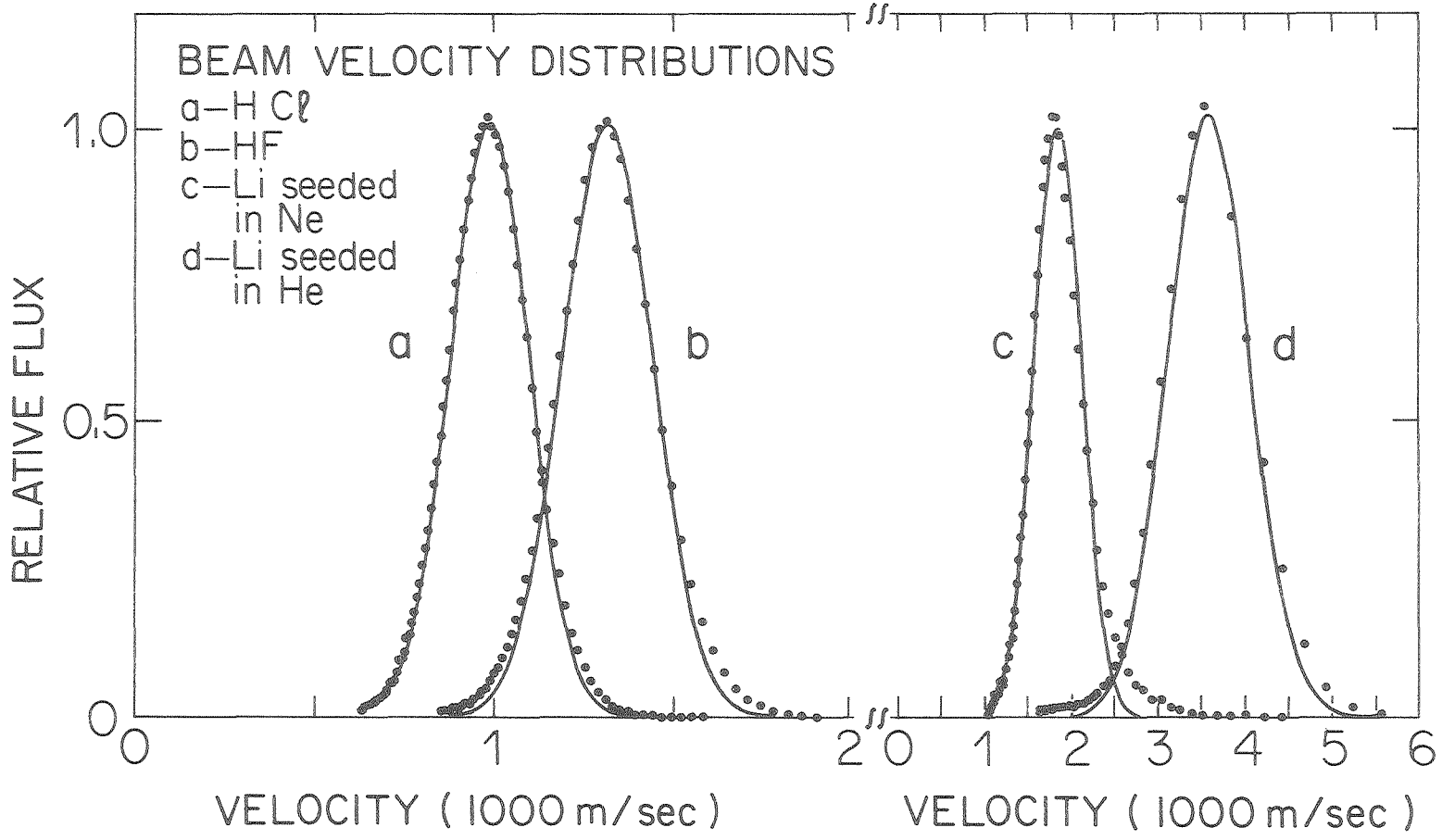

Fig. 1

XBL7910-4562

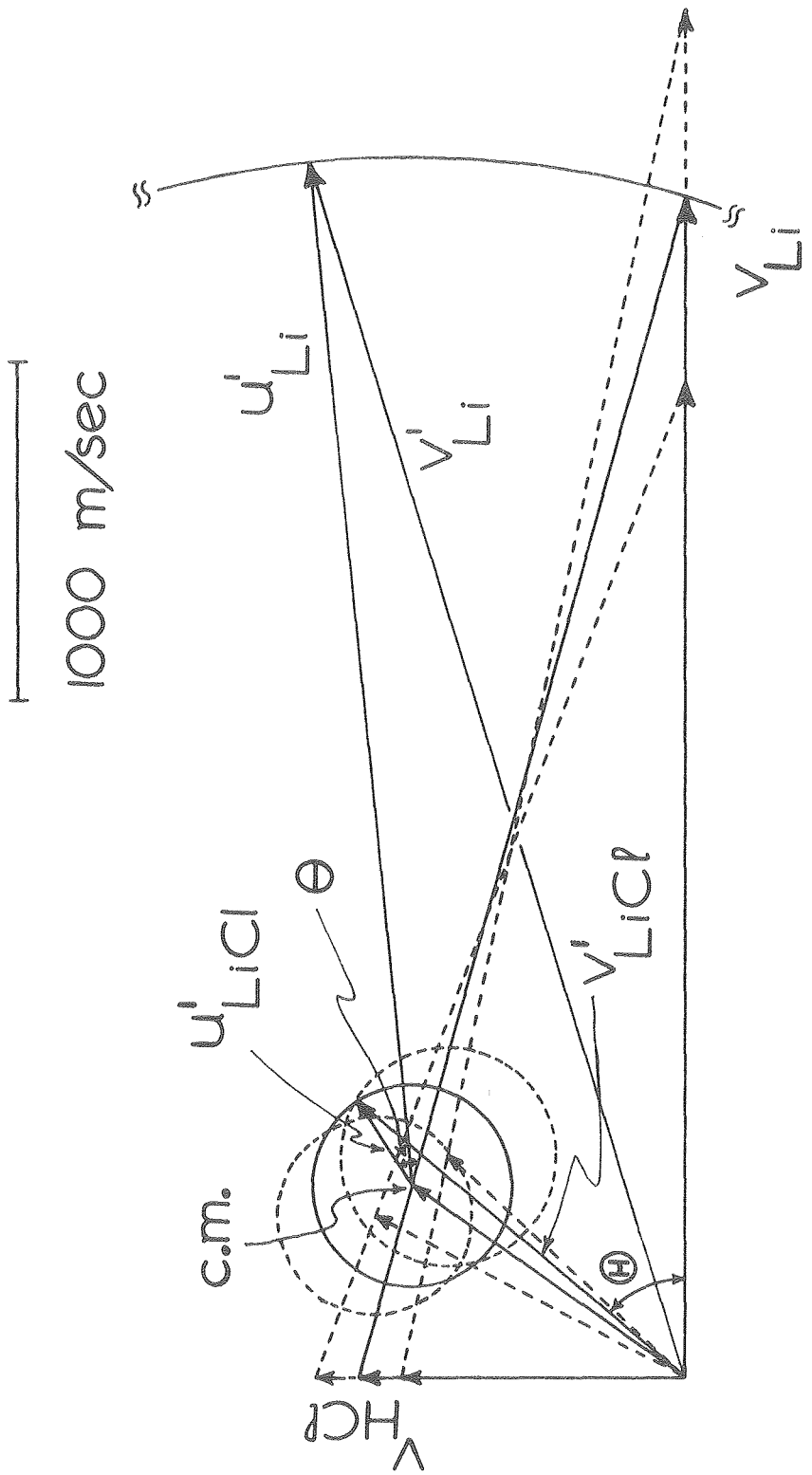

XBL 7911-12650

Fig. 2

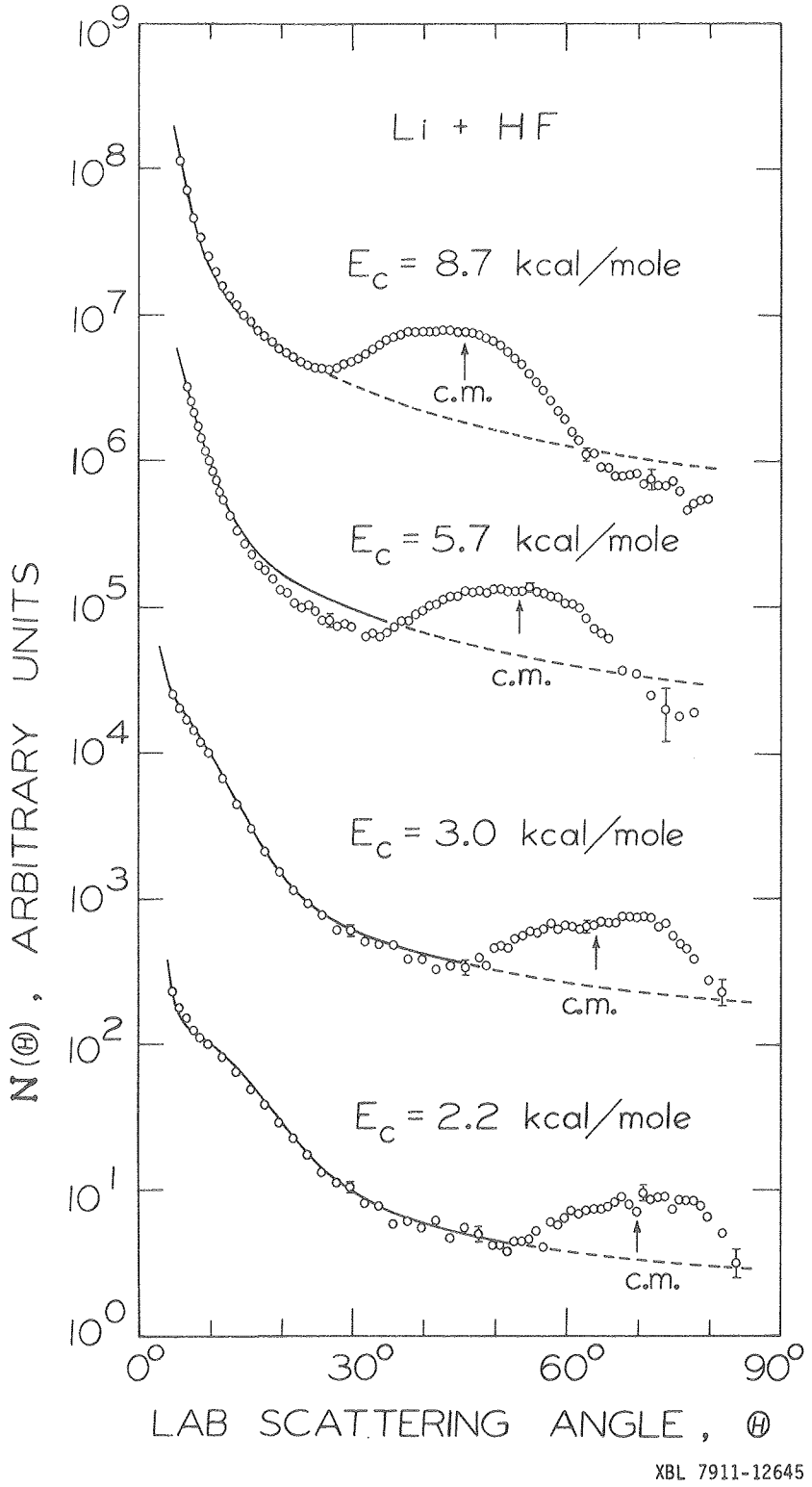
Li + HF
E_c = 8.7 kcal/mole
c.m.
E_c = 5.7 kcal/mole
c.m.
E_c = 3.0 kcal/mole
c.m.
E_c = 2.2 kcal/mole
c.m.
N(Θ), ARBITRARY UNITS
10^9
10^8
10^7
10^6
10^5
10^4
10^3
10^2
10^1
10^0
0°
30°
60°
90°
LAB SCATTERING ANGLE, Θ
XBL 7911-12645

Fig. 3

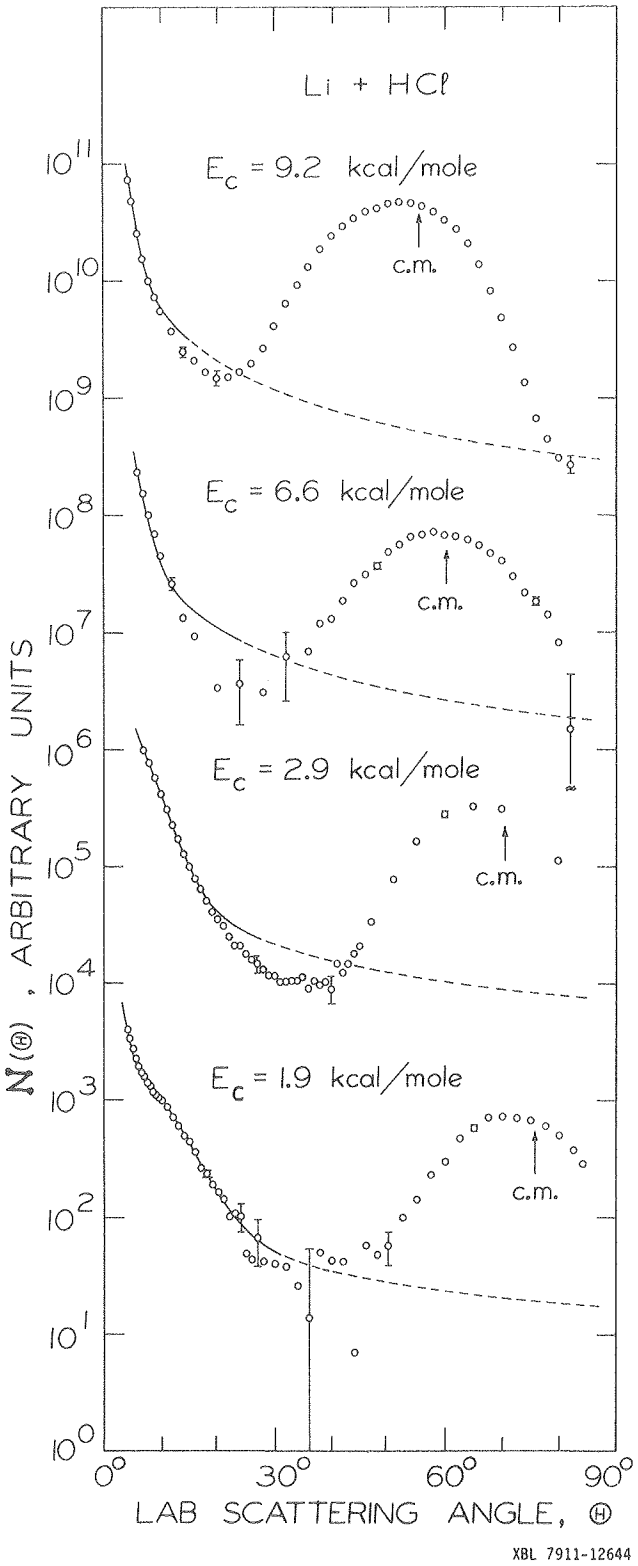
Li + HCl
E_c = 9.2 kcal/mole
E_c = 6.6 kcal/mole
E_c = 2.9 kcal/mole
E_c = 1.9 kcal/mole
c.m.
10^{11}
10^{10}
10^{9}
10^{8}
10^{7}
10^{6}
10^{5}
10^{4}
10^{3}
10^{2}
10^{1}
10^{0}
N(Θ), ARBITRARY UNITS
0°
30°
60°
90°
LAB SCATTERING ANGLE, Θ
XBL 7911-12644

Fig. 4

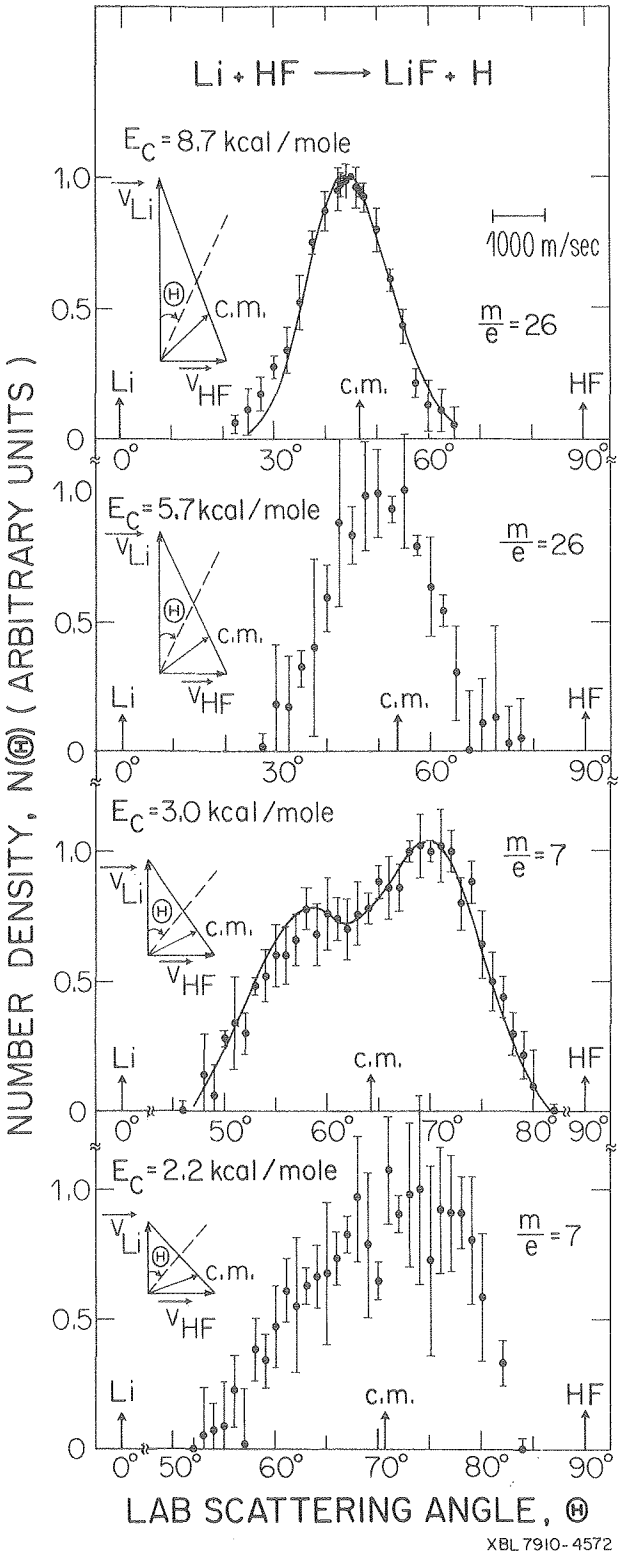
Li + HF ⟶ LiF + H
E_C = 8.7 kcal / mole
E_C = 5.7 kcal / mole
E_C = 3.0 kcal / mole
E_C = 2.2 kcal / mole
1000 m/sec
m/e = 26
m/e = 7
V_Li
V_HF
c.m.
Li
HF
NUMBER DENSITY, N(Θ) (ARBITRARY UNITS)
LAB SCATTERING ANGLE, Θ
XBL 7910-4572

Fig. 5

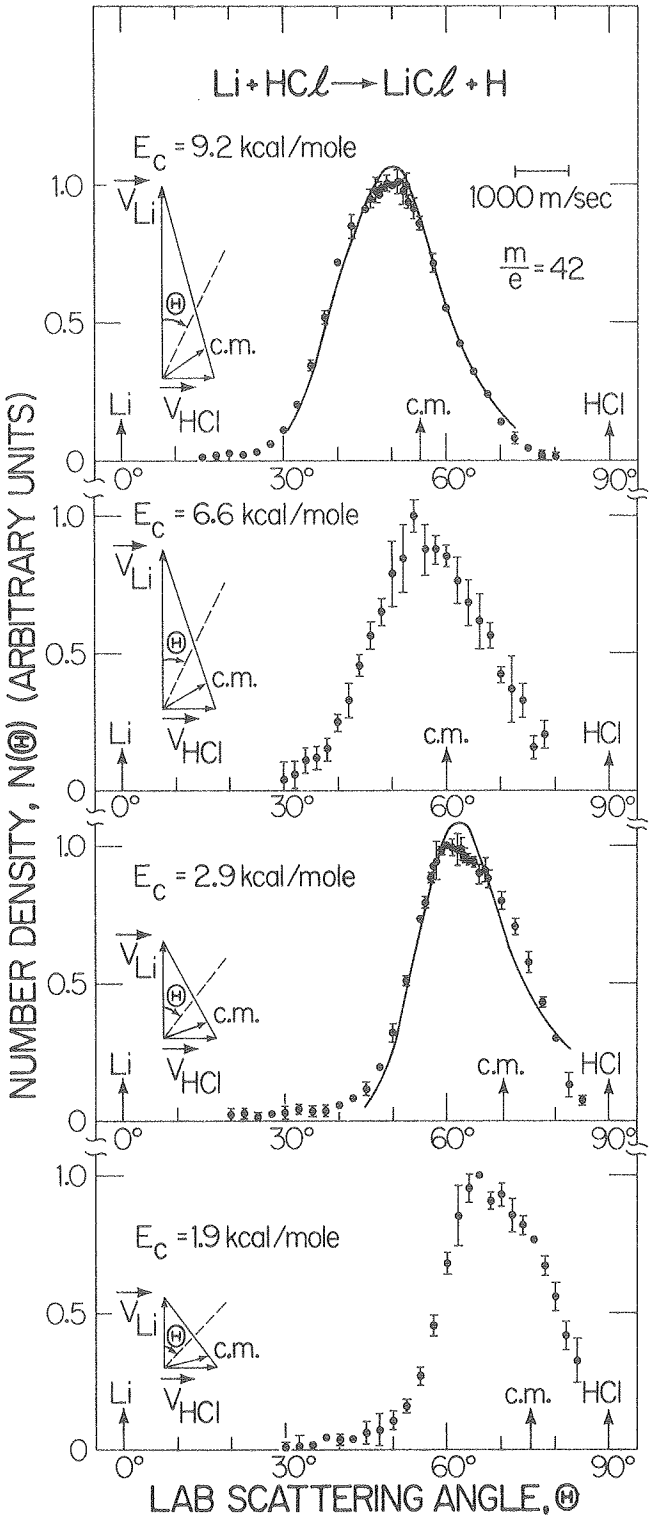

XBL 7910-4571

Fig. 6

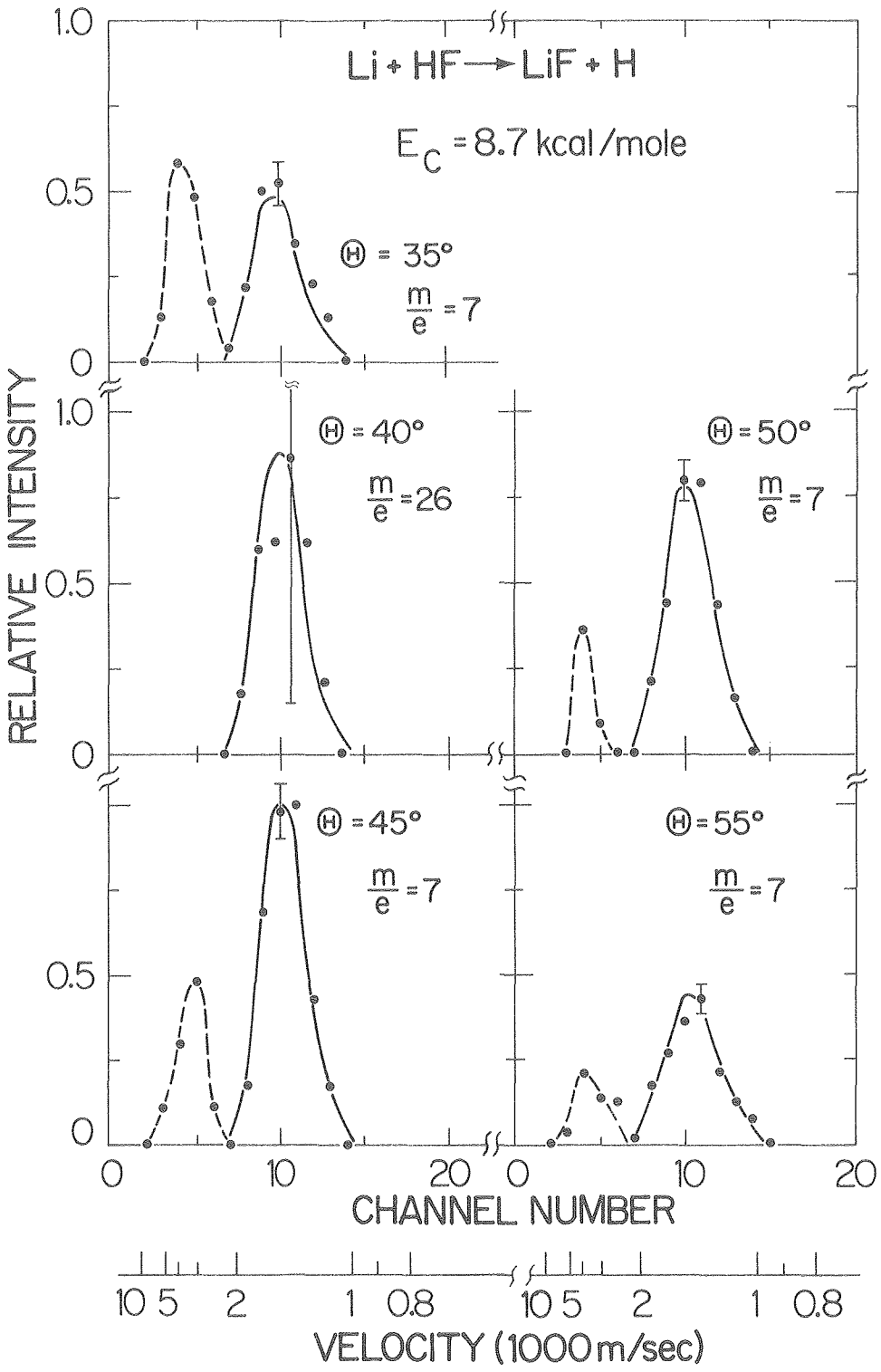
Li + HF → LiF + H
E_c = 8.7 kcal/mole
Θ = 35°
m/e = 7
Θ = 40°
m/e = 26
Θ = 50°
m/e = 7
Θ = 45°
m/e = 7
Θ = 55°
m/e = 7
RELATIVE INTENSITY
1.0
0.5
0
0
10
20
CHANNEL NUMBER
10 5 2 1 0.8
VELOCITY (1000 m/sec)
XBL 7911-12662

Fig. 7

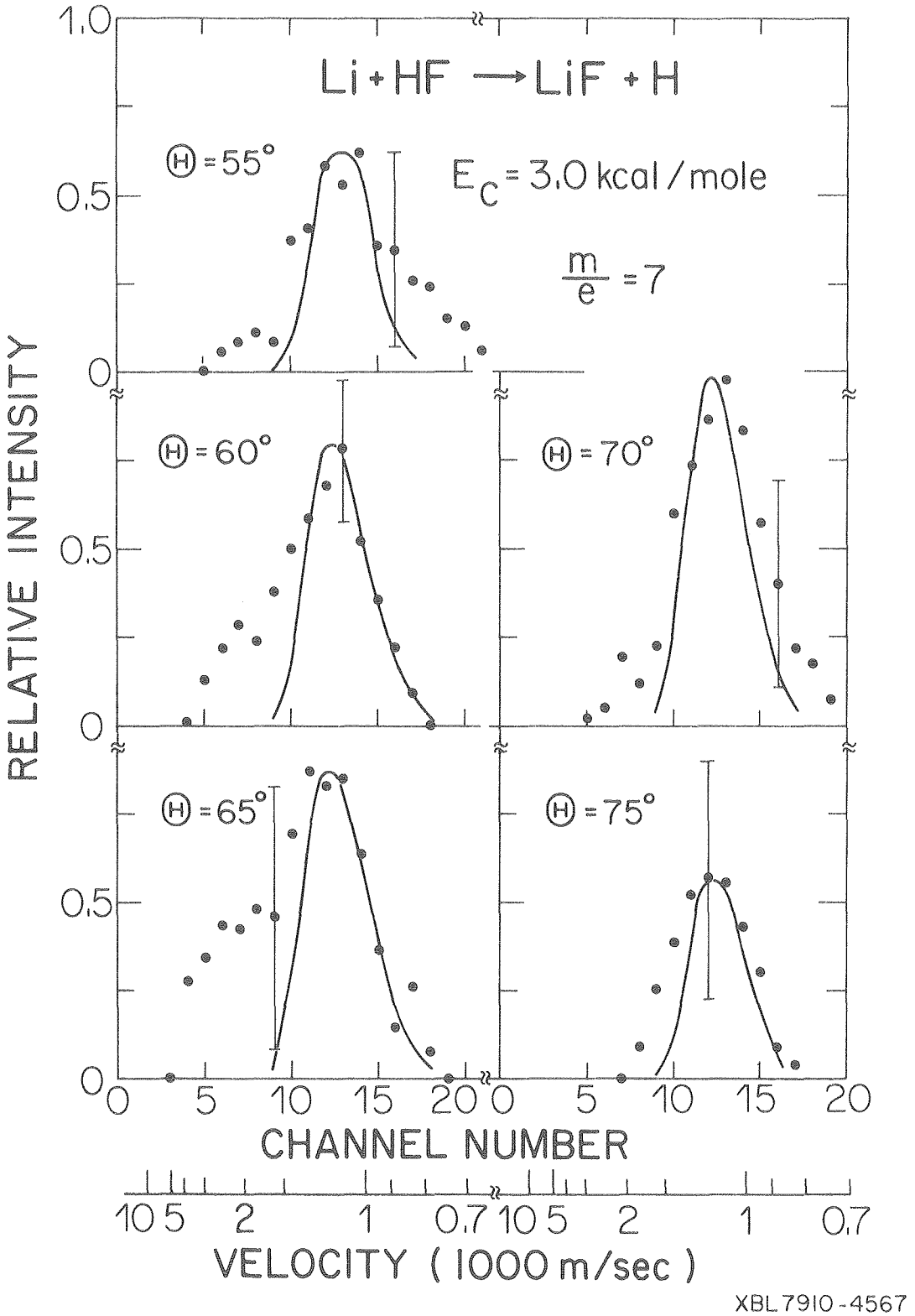
Li + HF → LiF + H
Ⓗ = 55°
E_c = 3.0 kcal / mole
$\frac{m}{e}$ = 7
Ⓗ = 60°
Ⓗ = 70°
Ⓗ = 65°
Ⓗ = 75°
RELATIVE INTENSITY
1.0
0.5
0
0 5 10 15 20
CHANNEL NUMBER
10 5 2 1 0.7
VELOCITY (1000 m/sec)
XBL 7910-4567

Fig. 8

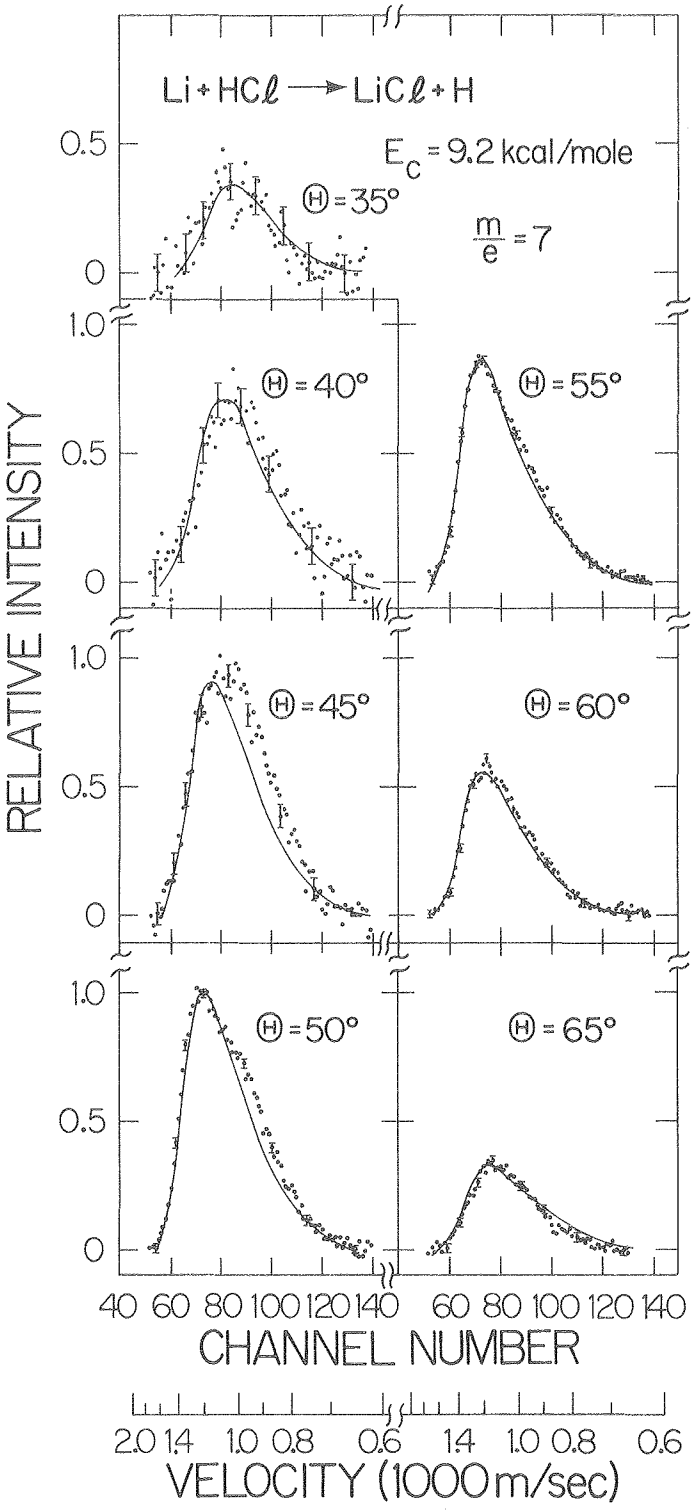

XBL 7911-12700

Fig. 9

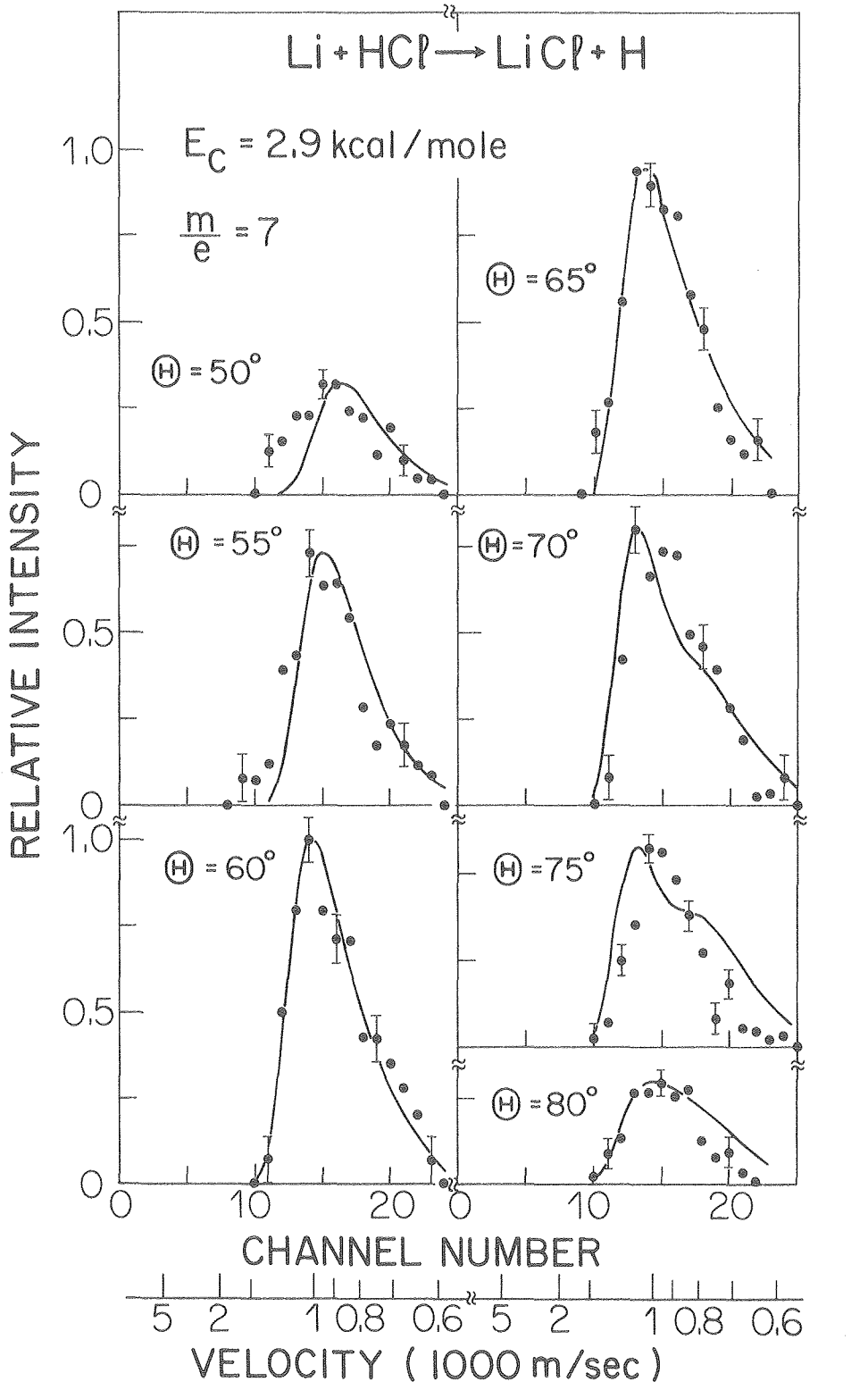

XBL 7910-4566

Fig. 10

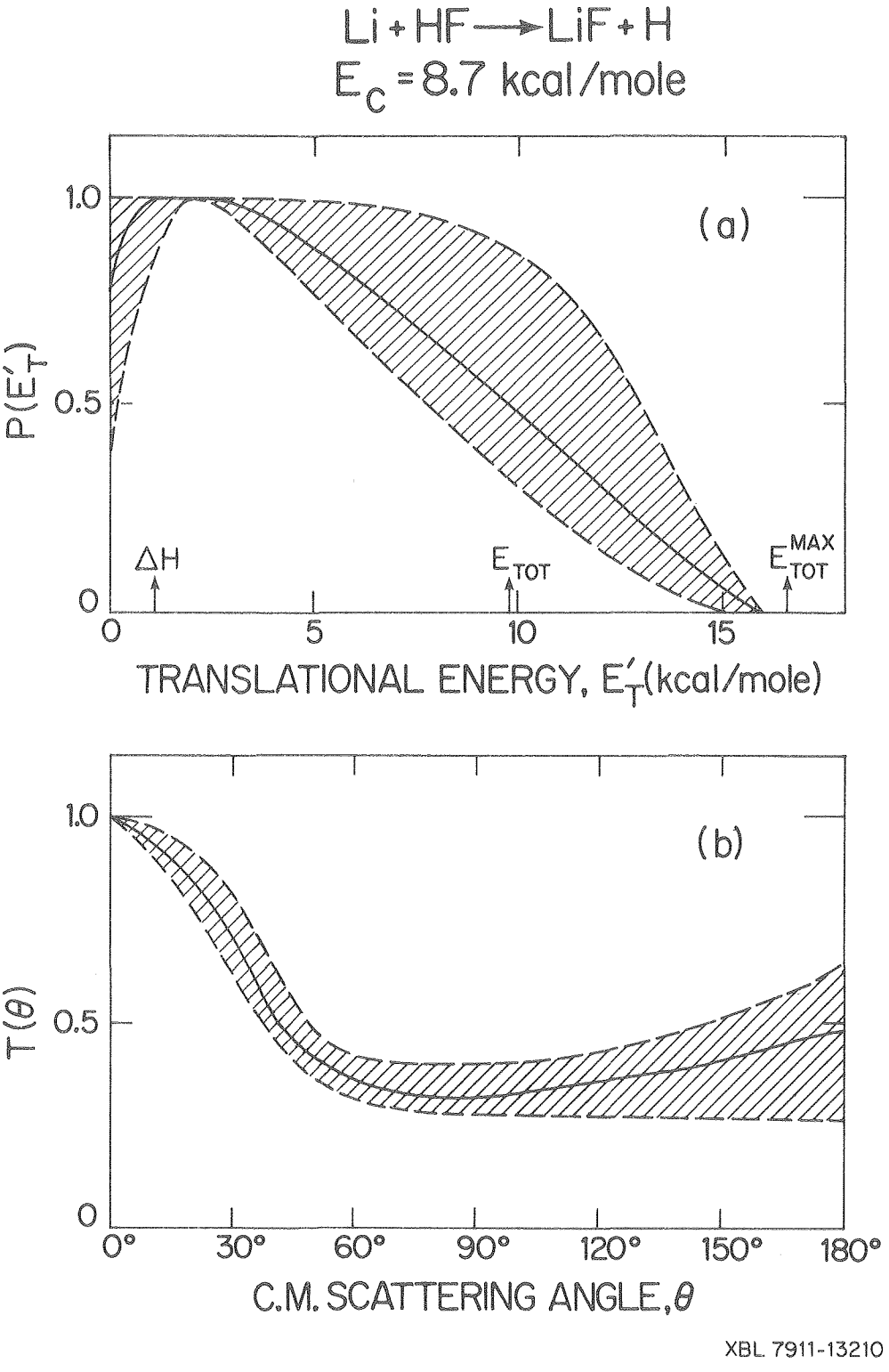
Li + HF ⟶ LiF + H
E_c = 8.7 kcal/mole
(a)
1.0
0.5
0
$P(E'_T)$
ΔH
E_{TOT}
E_{TOT}^{MAX}
0
5
10
15
TRANSLATIONAL ENERGY, E'_T(kcal/mole)
(b)
1.0
0.5
0
$T(\theta)$
0°
30°
60°
90°
120°
150°
180°
C.M. SCATTERING ANGLE, θ
XBL 7911-13210

Fig. 11

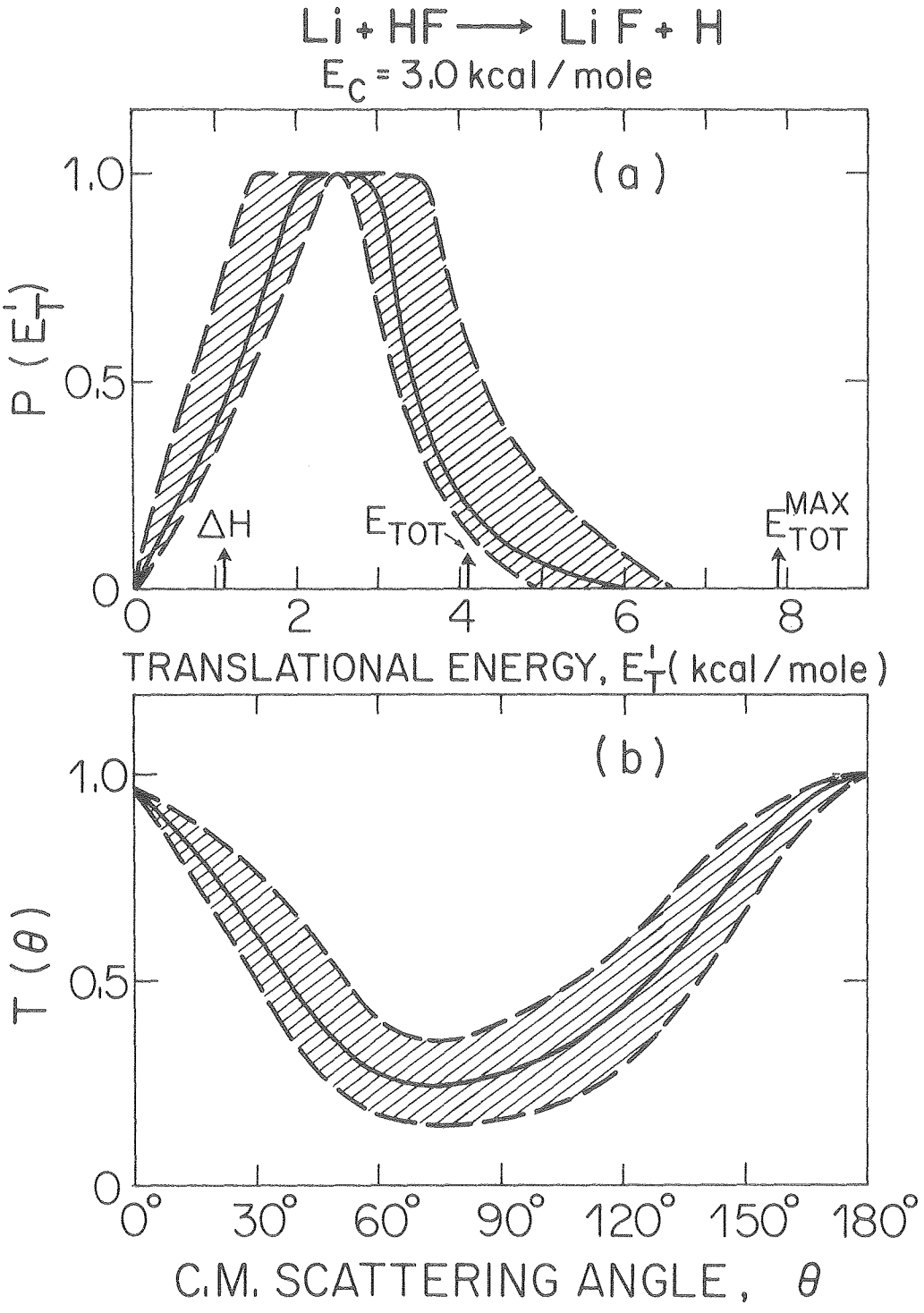

Fig. 12

XBL 7910-4565

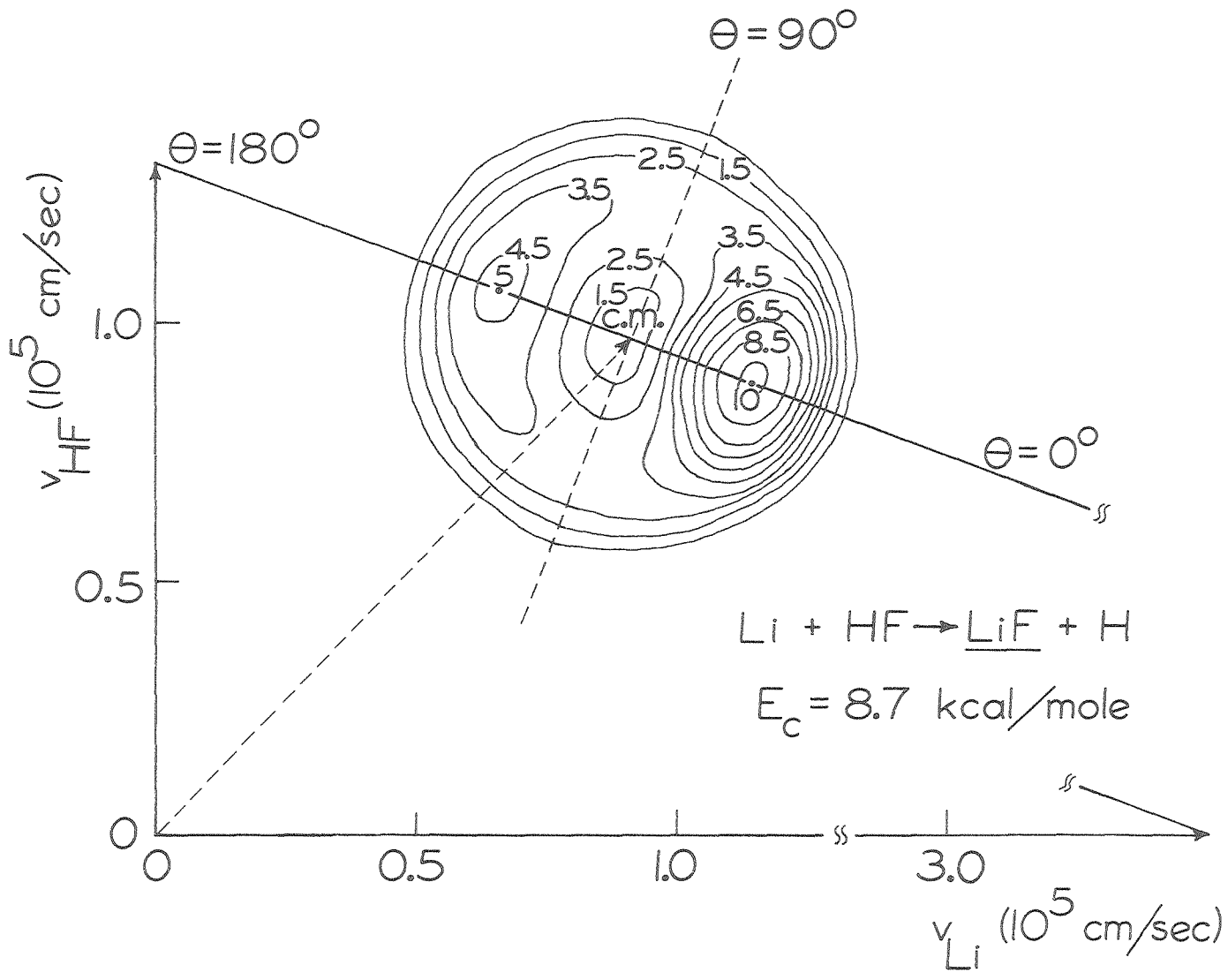

XBL 7911-12647

Fig. 13

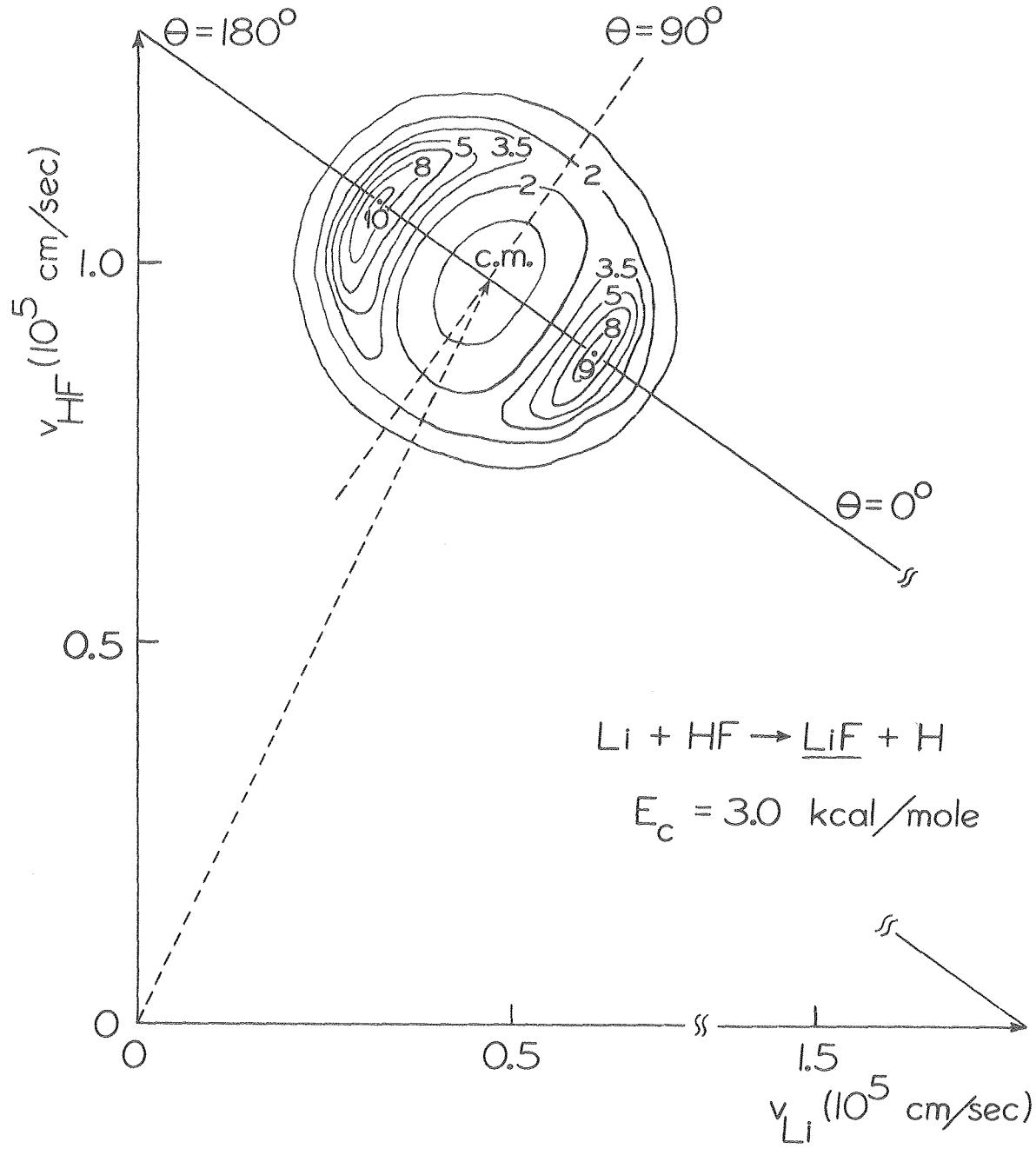

XBL 7911-12646

Fig. 14

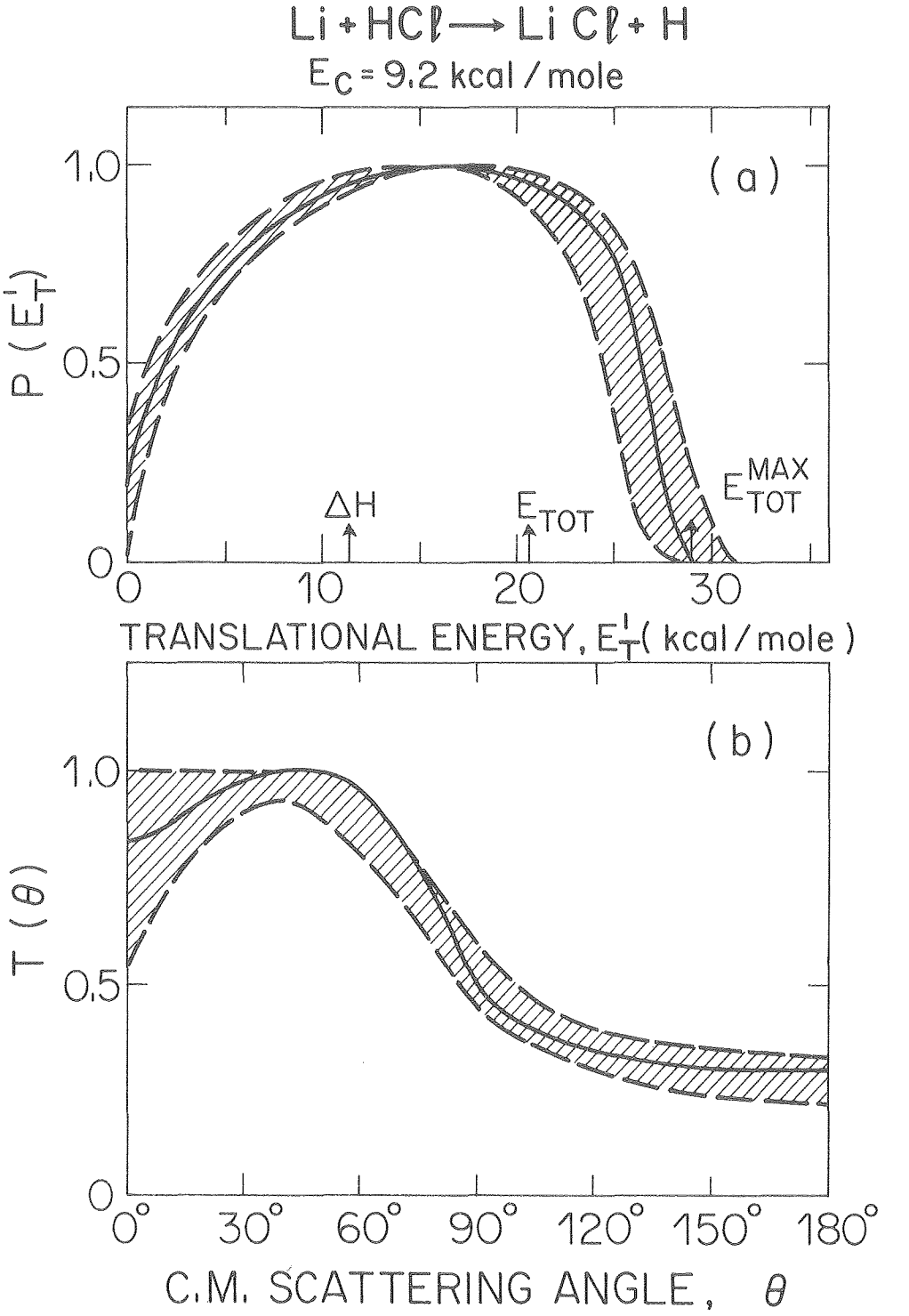

Fig. 15

XBL 7910-4573

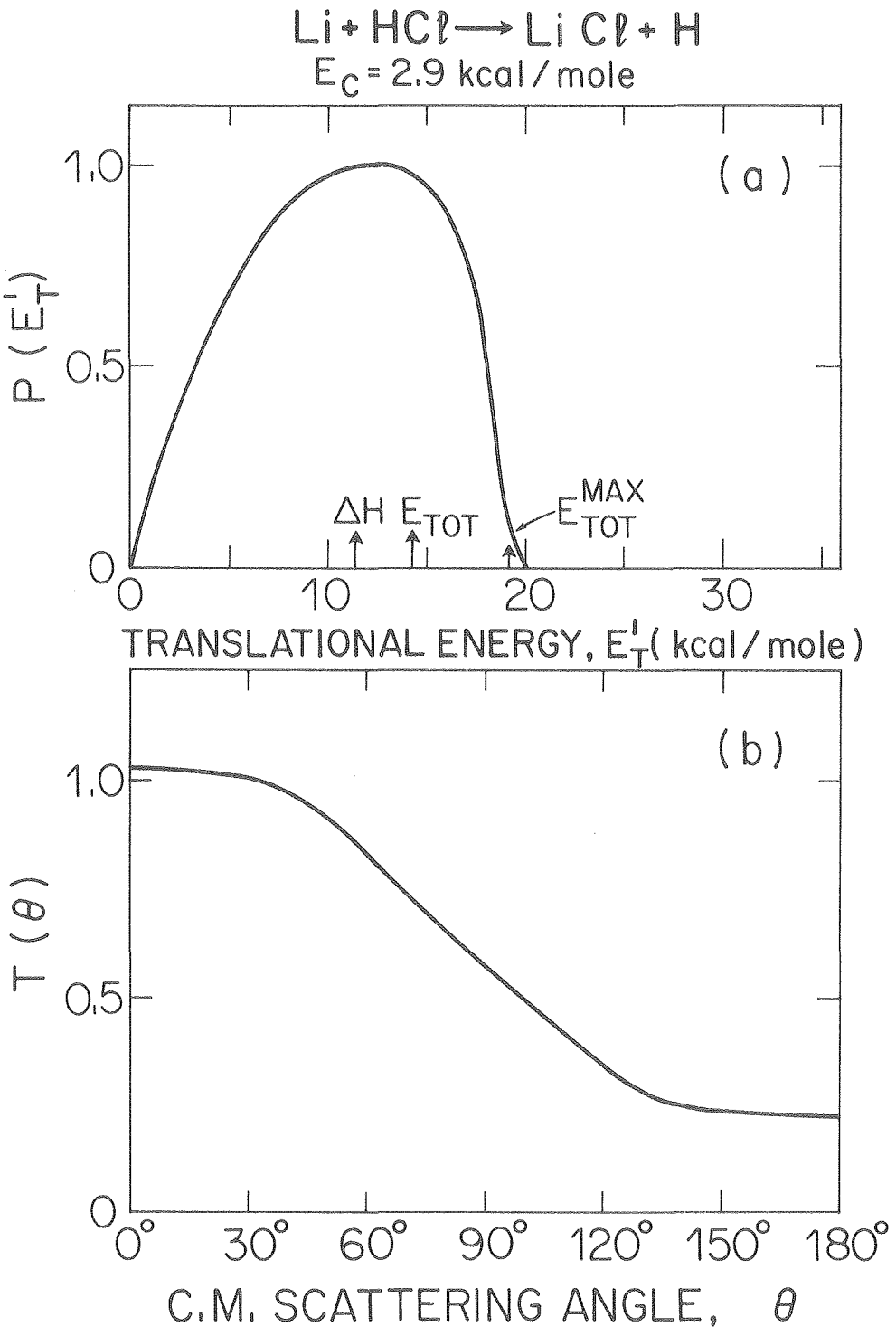

Fig. 16 XBL7910-4564

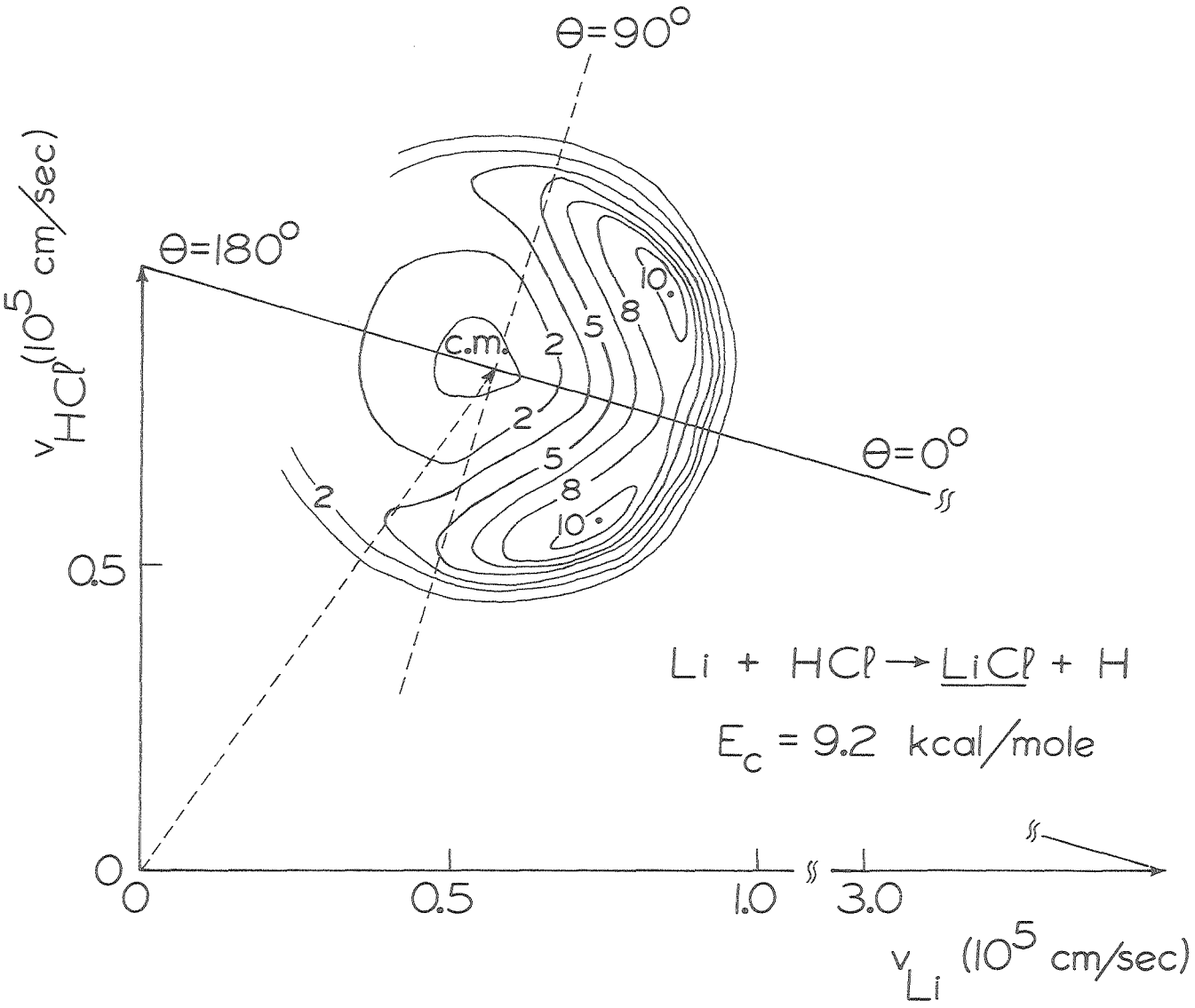

XBL 7911-12648

Fig. 17

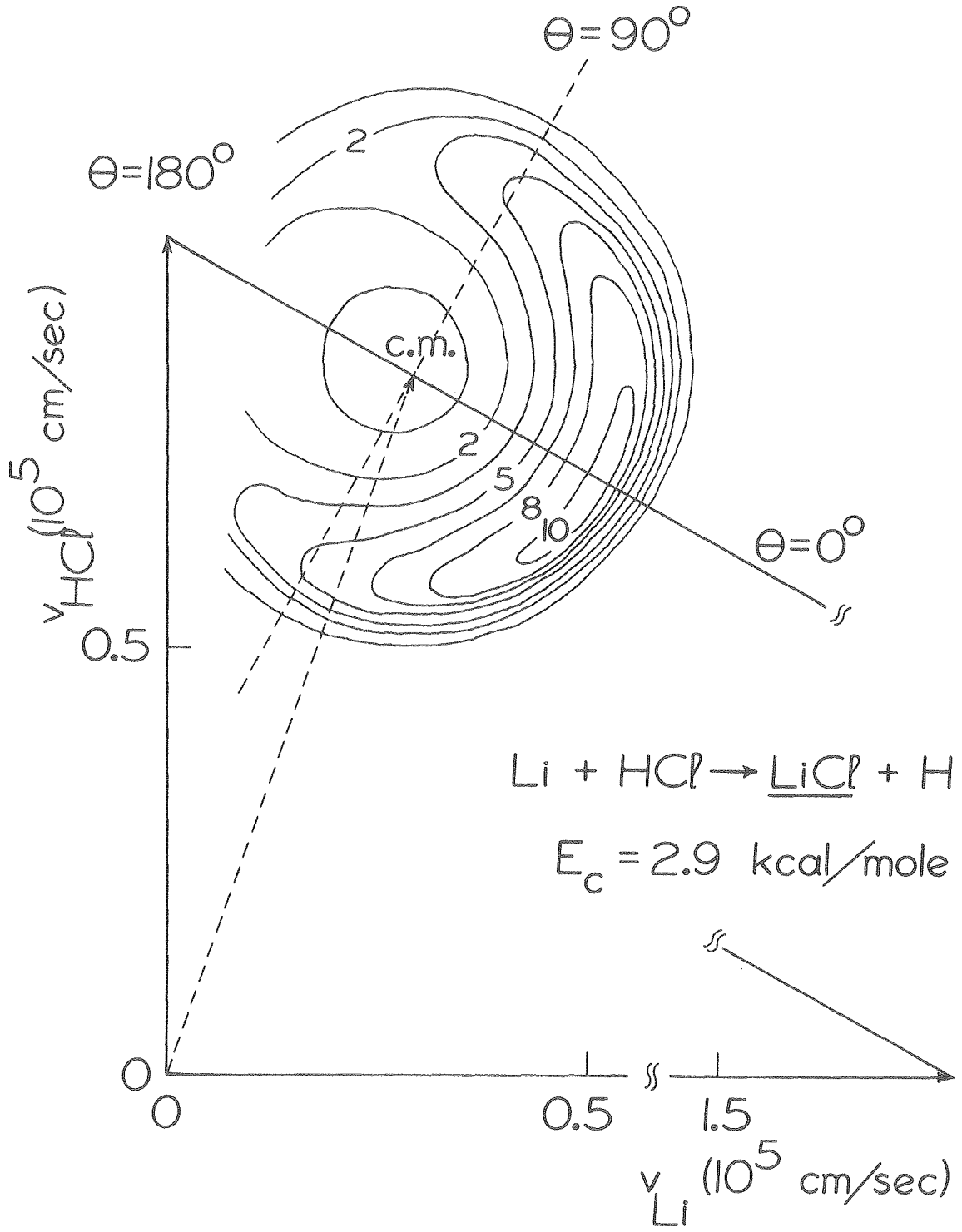

XBL 7911-12649

Fig. 18

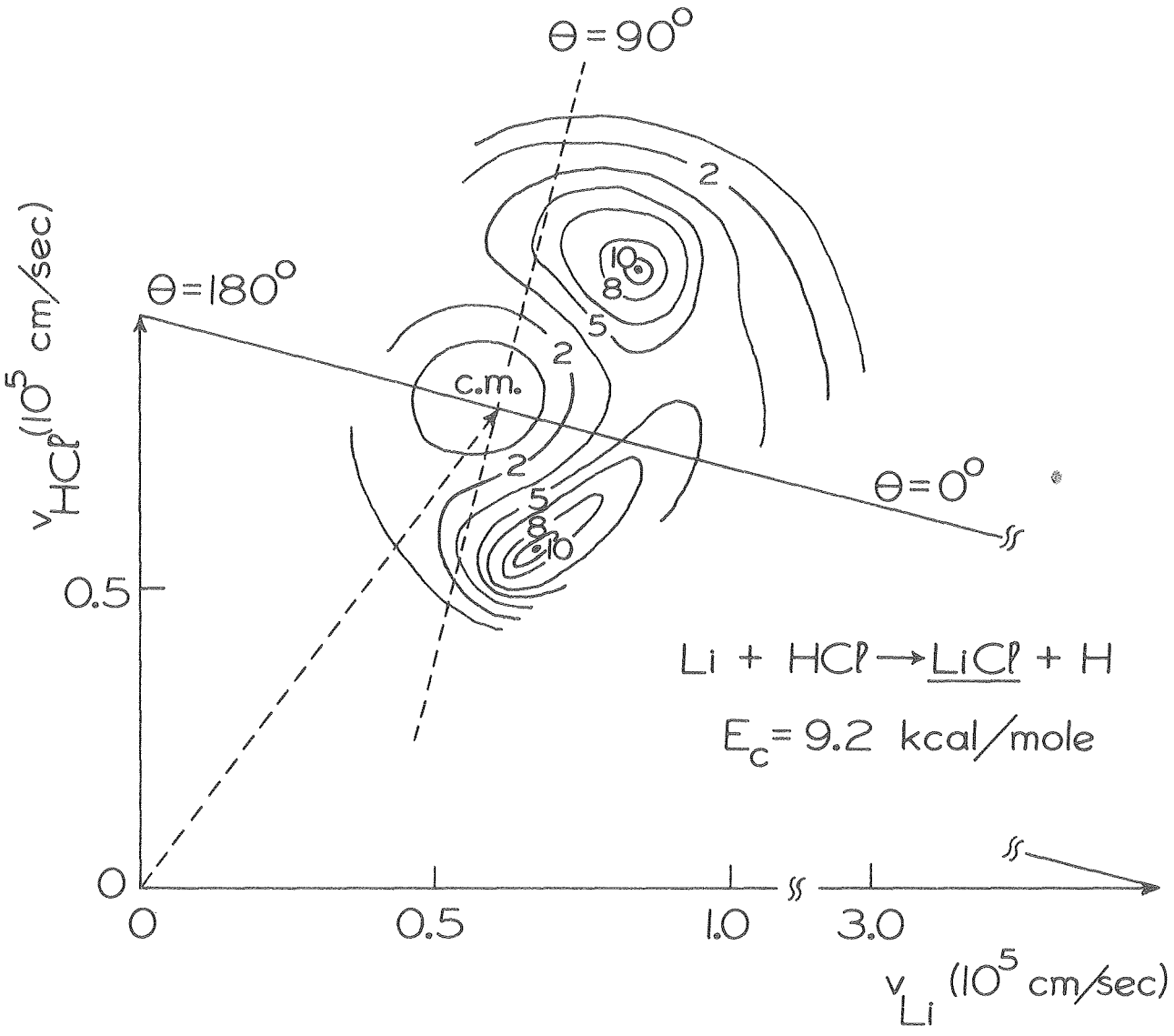
Θ = 90°
Θ = 180°
Θ = 0°
c.m.
2
5
8
10
v_{HCl} (10^5 cm/sec)
0.5
0
0.5
1.0
3.0
v_{Li} (10^5 cm/sec)
Li + HCl → LiCl + H
E_c = 9.2 kcal/mole
XBL 803-8424

Fig. 19

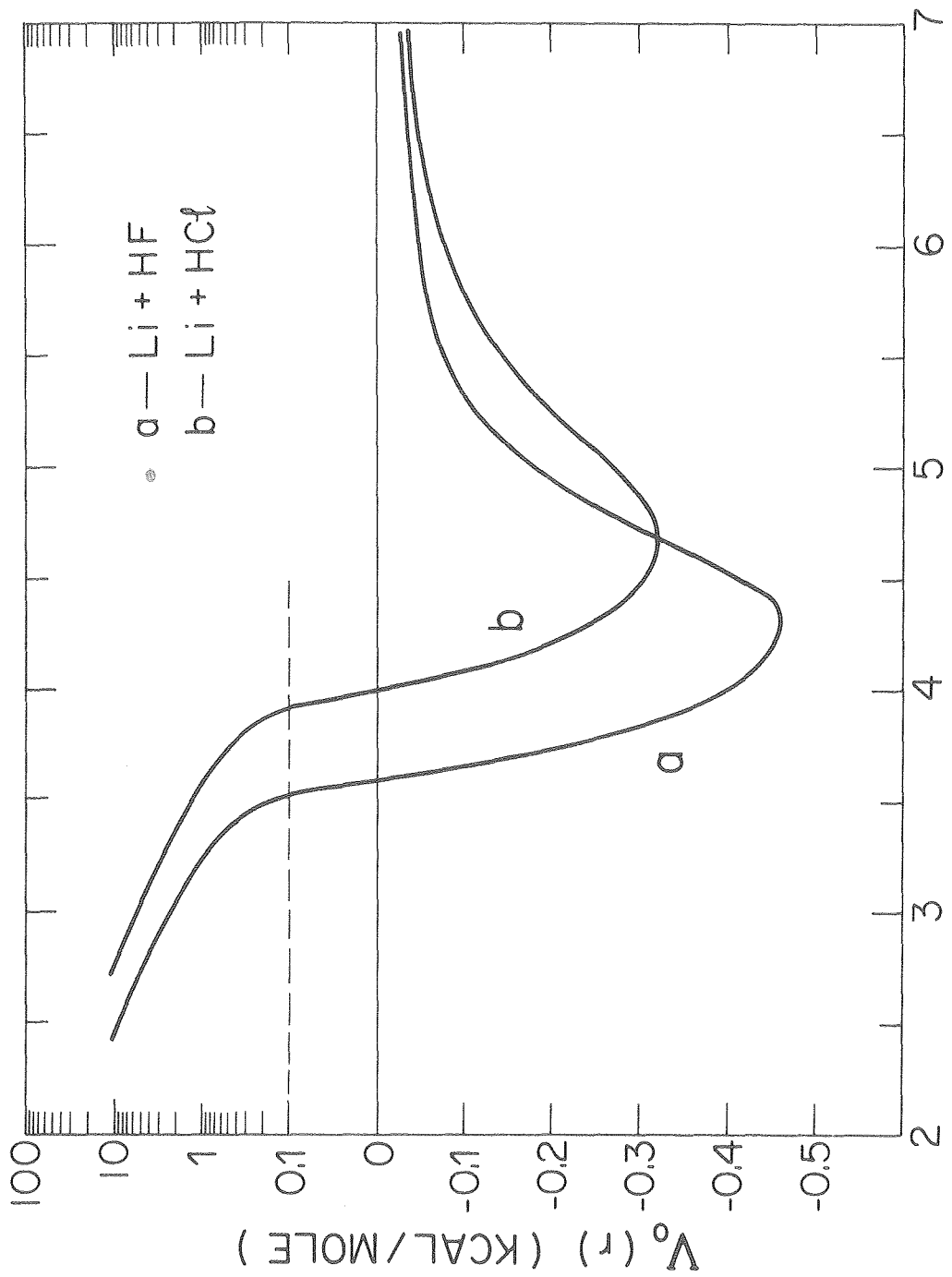

XBL 7910-4563

Fig. 20